Applied Catalysis B: Environmental 256 (2019) 117815

Contents lists available at ScienceDirect

Applied Catalysis B: Environmental

journal homepage: www.elsevier.com/locate/apcatb

Deactivation of Cu-SSZ-13 SCR catalysts by vapor-phase phosphorus exposure

Kunpeng Xie[a], Aiyong Wang[a], Jungwon Woo[a], Ashok Kumar[b], Krishna Kamasamudram[b], Louise Olsson[a,*]

[a] Competence Centre for Catalysis, Chemical Engineering, Chalmers University of Technology, Gothenburg, SE, 412 96, Sweden
[b] Cummins Inc., 1900 McKinley Avenue, MC 50183, Columbus, IN, 47201, USA

ARTICLE INFO

Keywords:
Cu-SSZ-13
Ammonia SCR
Zeolite catalyst
Catalyst deactivation
Phosphorus poisoning

ABSTRACT

Phosphorus in vehicle exhaust is one of the typical derivatives from fuels and lubricant oils that cause irreversible deactivation of automotive catalysts. In this work, we investigate the deactivation of Cu-SSZ-13 by vapor-phase phosphorus poisoning (100 ppm H_3PO_4) under NH_3-free lean conditions and NH_3-SCR operating conditions. The poisoned monolith catalysts were characterized with XPS, ICP-SFMS, SEM-EDX mapping, and H_2-TPR. The influence of phosphorus on catalytic performance (i.e. standard NH_3-SCR, NH_3 oxidation, NO oxidation, NH_3 storage, and NO storage) was evaluated. Phosphorus is mainly stored in the form of metaphosphate in poisoned catalysts, and it possesses axial and radial gradients on catalyst washcoats. Phosphorus strongly affects the copper reduction property, as revealed by the shifts in copper reduction to higher temperature in H_2-TPR experiments. Variations in phosphorus poisoning conditions are found to mainly impact the amounts of phosphorus captured and stored in the monolith catalysts. In order to elucidate the deactivation mechanism, the deactivation is correlated with the P/Cu ratio. The temperature shift for copper reduction significantly increases with the P/Cu ratio and levels at high Cu/P ratios. The deactivation degrees of NH_3 oxidation and NO oxidation as a function of the P/Cu ratio follow the same trend as the copper reduction temperature. This is possibly due to the formation of copper phosphates in the large cages, which deactivates the copper sites for NH_3 and NO oxidation. The deactivation for standard NH_3-SCR, NH_3 storage, and NO storage is proportional to the P/Cu ratio. The impact of phosphorus on NO storage is significantly stronger than on NH_3 storage, indicating that greater contribution to deactivation is brought about by the decreased capacity of NO chemisorption.

1. Introduction

Currently, the selective catalytic reduction (SCR) of nitrogen oxides (NO_x) with ammonia (NH_3-SCR) is being developed as a leading deNO_x technique for the after-treatment of commercial engine-powered vehicles to meet stringent emission legislations [1–5]. An efficient and robust NH_3-SCR catalyst must meet at least three requirements: high NO_x conversion over a relatively wide temperature window, hydrothermal stability, and tolerance to poisons (e.g. hydrocarbons, sulfur, phosphorus, alkali metals, and alkaline earth metals.). Vanadium-based mixed oxides (e.g. V_2O_5-WO_3/TiO_2) are the first generation of NH_3-SCR catalysts used for heavy-duty vehicles. However, the instability of the TiO_2 support and the possibility of the formation of volatile vanadium species are concerns with these catalysts [6]. Subsequently, metal-exchanged zeolite catalysts (mainly Cu- and Fe-based zeolites) have shown improved SCR activity over a wider operating temperature window and higher hydrothermal stability [7,8], and, thus, they are now commonly used as NH_3-SCR catalysts for heavy-duty, medium-duty, and light-duty vehicles. A variety of zeolites have been extensively studied as NH_3-SCR catalysts, for instance, ZSM-5, Y-zeolite, beta, and chabazite. Recently, Cu/CHA, for example Cu-SSZ-13, with a small-pore microporous structure, has gained interest among various zeolite catalysts. This has resulted in extensive practical and fundamental studies in the automotive catalysis community due to its high activity at low temperatures and high hydrothermal stability under NH_3-SCR conditions [9–13].

Besides the SCR performance and hydrothermal stability, improving the tolerance of SCR catalysts to poisoning by the contaminants in the exhaust from diesel or gas engine, aqueous urea solution, and volatile precious metals from diesel oxidation catalysts [14] remains a

* Corresponding author.
E-mail address: louise.olsson@chalmers.se (L. Olsson).

https://doi.org/10.1016/j.apcatb.2019.117815
Received 20 December 2018; Received in revised form 29 April 2019; Accepted 2 June 2019
Available online 03 June 2019
0926-3373/

challenge in SCR technology. The poisoning of SCR catalysts can be very complicated. The contaminants in the exhaust can be derived from impurities in diesel or gas fuels or from volatile engine oils and fuel additives. Sulfur is a typical impurity in diesel fuel, whereas biofuels sometimes contain many types of impurities (e.g. sulfur, phosphorus, alkali metals, and alkaline metals) at various concentrations [15]. The volatile engine oils (e.g. lubricant ZDDP, zinc diakyl dithio phosphates) and fuel additives (e.g. Akyl polyphosphoric acids) are also typical sources of P, S, and Zn in vehicular exhaust [16–18]. Phosphorus poisoning, in particular, can cause irreversible catalyst deactivation and, thus, this has been considered to be detrimental to SCR catalysts due to difficulties in catalyst regeneration [18–20]. Dahlin and co-workers [21] examined Euro V (vanadia SCR only) and Euro VI (DOC + DPF + SCR) vehicle-aged systems. They found P on the SCR catalyst in the Euro V system and also some on the SCR catalyst in the Euro VI system. Shibata et al. [22] studied a DOC + SCR system and found phosphorous also in the inlet of the SCR catalyst and that the amount was dependent on the lubricant oil type. Eaton et al. [23] found about 2% P in the outlet of a field returned DOC (after 1.5 years in operation). These results suggest, that since it is such a large amount of phosphorus in the outlet part of the DOC that it is a risk that phosphorus also can reach the SCR component, especially if an SCR coated filter is used directly after the DOC. Field-aged Euro IV system using two vanadia SCR bricks showed substantial amount of phosphorus also on the second brick, which clearly shows that P can interact with more catalysts than the first in the system [24]. Therefore, it is very important to in-depth investigate the phosphorus poisoning mechanism on the state-of-the-art Cu-SSZ-13 catalysts, which have been applied in Europe and USA-based markets. There are mainly two approaches to phosphorus poisoning reported in the literature: wet impregnation with H_3PO_4 [25,26] or phosphate solutions [27,28] followed by calcination at elevated temperatures and gas-phase treatment with vaporized H_3PO_4 [29,30] or $(NH_4)_2HPO_4$ [31,32] under lean conditions.

Compared to sulfur poisoning on Cu-SSZ-13 catalysts, which has already been extensively investigated in the literature [33–37], Phosphorus poisoning has not yet been well studied and the poisoning mechanism has not been fully understood. Only a few studies have examined phosphorus poisoning on Cu-SSZ-13, where the poisoning experiments were performed with conventional incipient wetness impregnation using $(NH_4)_2HPO_4$ solutions as precursors [38–41]. Despite the convenience and easy control of poison dose, it is also important to study phosphorus poisoning under operating conditions closer to a real catalyst system, where the catalyst is exposed to phosphorus species in the gas phase. Toops and coworkers have found that the phosphorus derived from the combustion of ZDDP in a diesel engine was mainly in the form of phosphoric acid (H_3PO_4) [17]. Therefore, implementing poisoning with H_3PO_4 in the gas phase is believed to reflect the practical characteristics of catalyst poisoning with phosphorus. For instance, Shwan et al. and Andonova et al., respectively, have reported on phosphorus poisoning of large-pore Fe/BEA and Cu/BEA catalysts by exposing the washcoated monoliths to H_3PO_4-containing exhaust gas under hydrothermal lean conditions [29,42].

However, to the best of our knowledge, there are no studies that report on phosphorus poisoning of small-pore Cu-SSZ-13 using vapor-phase poisoning. In this work, we, therefore, simulated the phosphorus poisoning of Cu-SSZ-13 washcoated monolith catalysts by exposing them to H_3PO_4-containing exhaust under lean hydrothermal conditions in the absence of NH_3 and NO, i.e. 100 ppm H_3PO_4, 5 vol.% H_2O, 8 vol.% O_2 in Ar, 160–400 °C. Two key parameters, poisoning temperature and duration, were investigated. In addition, for the first time, we simulated the phosphorus poisoning of Cu-SSZ-13 washcoated monolith catalysts by exposing them to H_3PO_4-containing exhaust under NH_3-SCR operating conditions, i.e. 100 ppm H_3PO_4, 400 ppm NH_3, 400 ppm NO, 5 vol.% H_2O, 8 vol.% O_2 in Ar, 200–400 °C. The influence of phosphorus on the catalytic performance of Cu-SSZ-13 washcoated monolith catalysts was evaluated by comparing the catalytic activities of the monolith catalysts before and after poisoning. The poisoned monolith catalysts were characterized with ICP-SFMS, SEM-EDX mapping, H_2-TPR, and XPS.

2. Experimental methods

2.1. Catalyst preparation

Cu-SSZ-13 (SiO_2/Al_2O_3 ratio of 11.2, Cu loading of 4.4 wt.%, and ion-exchange level of 0.42Cu/Al) catalysts were prepared according to procedures described elsewhere [12,13]. Zeolite Y (CBV712, Zeolyst International) was used for the hydrothermal synthesis of Na-SSZ-13. To simulate poisoning in the vapor phase, the obtained powder catalysts were washcoated onto cordierite monoliths (L = 20 mm, D = 14.4 mm, cell density = 400 cpsi) [39]. Prior to the washcoating, the monoliths were cleaned in air atmosphere for 2 h at 500 °C. Boehmite (Disperal D, Sasol GmbH) was used as binder. A slurry prepared for washcoating was composed of 20 wt.% solid and 80 wt.% liquid. The solid phase contained 95 wt.% Cu-SSZ-13 and 5 wt.% boehmite, and the liquid phase consisted of 50 wt.% distilled water and 50 wt.% ethanol. Each monolith was coated repeatedly until it reached the desired amount of washcoat (˜ 300 mg) and, subsequently, calcined for 2 h at 500 °C in air atmosphere.

2.2. Catalytic activity measurements and phosphorus poisoning of monolith catalysts in flow reactor

The catalytic activity of the monolith catalysts was measured in a flow reactor setup using a horizontal tube with a length of 700 mm and an inner diameter of 16 mm. A LabVIEW interface was used to control the flow setup system. The gas flows were regulated with mass flow controllers (MFC, Bronkhorst), and the water vapor was dosed with an evaporation mixing system (CEM, Bronkhorst) working under an evaporation temperature of 110 °C. The gases and water vapor were mixed before being fed into the reactor, and all gas lines including the exhaust line were heated to 191 °C. Argon was used as the inert balance in order to achieve a total flow of 1200 ml min^{-1} (space velocity 22,100 h^{-1} based on monolith volume) for all experiments. The monolith catalysts were placed in the downstream of the tube reactor (about 80 mm from the reactor outlet). A thermocouple was positioned about 10 mm in front of the monolith for measuring/controlling the reactor temperature, and a second one was placed in the center of the monolith for monitoring the catalyst temperature. The concentrations of the gases (i.e. NH_3, NO, N_2O, NO_2 and H_2O) in the exhaust stream were monitored online using an MKS Multigas 2030 FTIR spectrometer.

An experimental procedure for the evaluation of the phosphorus poisoning effect on Cu-SSZ-13 monolith catalysts is depicted in Scheme 1. The catalytic activity (standard SCR, NH_3 oxidation, NO oxidation and NH_3-TPD) of each monolith catalyst was always evaluated before and after phosphorus poisoning on the same monolith to ensure that the differences observed were from the poisoning.

2.2.1. Catalytic activity measurements in flow reactor

Prior to the catalytic activity test, each fresh monolith catalyst was degreened with a gas mixture of 400 ppm NH_3, 400 ppm NO, 8 vol.%O_2, 5 vol.% H_2O and Ar for 3 h at 650 °C to stabilize the catalytic behaviors. Then the catalyst was pre-treated with 8 vol.% O_2, 5 vol.% H_2O and Ar as balance for 20 min at 650 °C before each experiment, including the experiments on the phosphorus-poisoned samples.

2.2.1.1. Standard NH_3-SCR. The reactor temperature was first stabilized at 80 °C and maintained at the same temperature for 90 min and, simultaneously, the feeding gas mixture was switched to 400 ppm NH_3, 400 ppm NO, 8 vol.% O_2, 5 vol.% H_2O and Ar. Then the reactor temperature was stepwise increased up to 150 °C with a 10 °C increment and a duration of 30 min per step in order to determine the

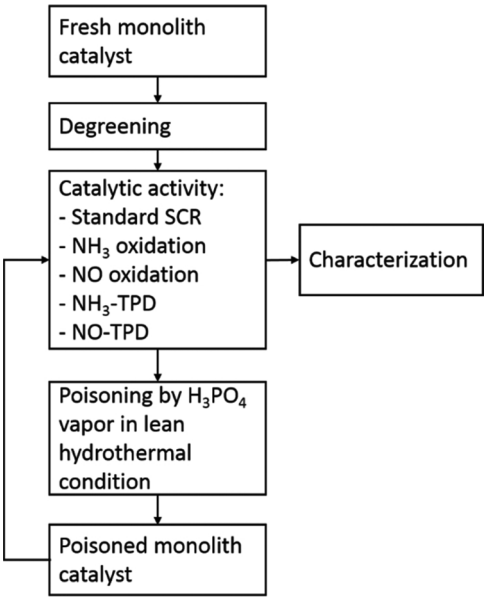

Scheme 1. Experimental procedure for evaluation of phosphorus poisoning effect on Cu-SSZ-13 monolith catalysts.

reaction rate with low NO_x conversion. Thereafter, the reactor temperature was further increased to 175, 200, 250, 300, 350, 400, and 500 °C with a duration of 30 min per step to measure the steady-state catalytic activity in a wide temperature window. A heating rate of 20 °C min^{-1} between each temperature step was always used.

2.2.1.2. NH_3 oxidation. The catalyst was exposed to 400 ppm NH_3, 8 vol.% O_2, 5 vol.% H_2O and Ar. After being maintained at 200 °C for 60 min, the reactor temperature was increased stepwise up to 300 °C with 10 °C steps and a duration of 30 min at each temperature in order to determine the reaction rate with low NH_3 conversion. Thereafter, the reactor temperature was further increased up to 500 °C with temperature steps of 50 °C and a duration of 30 min per step to measure the steady-state catalytic activity in a broad temperature interval. A heating rate of 20 °C min^{-1} between each step was applied.

2.2.1.3. NO oxidation. The catalyst was exposed to 400 ppm NO, 8 vol.% O_2, 5 vol.% H_2O and Ar at 200 °C. After being maintained at 200 °C for 30–60 min, the reactor temperature was increased stepwise up to 500 °C with 50 °C steps and a duration of 30 min per temperature in order to determine the steady-state NO oxidation activity in a wide temperature window. A heating rate of 20 °C min^{-1} between each step was used.

2.2.1.4. NO-TPD. NO-TPD was performed in dry conditions in order to avoid water inhibition. A total flow of 300 ml min^{-1} was used. The catalyst was exposed to 1500 ppm NO and Ar at 50 °C for 62 min to fully saturate the catalyst with NO. Subsequently, the reactor was purged with only Ar for 60 min at the same temperature and then heated up to 500 °C in the same gas flow with a ramp rate of 10 °C min^{-1} and then held at the same temperature for 20 min before cooling down.

2.2.1.5. NH_3-TPD. The catalyst was exposed to 400 ppm NH_3, 5 vol.% H_2O and Ar at 100 °C for 120 min to fully saturate the catalyst with NH_3. Subsequently, the reactor was purged with 5 vol.% H_2O and Ar for 60 min at the same temperature and then heated up to 500 °C in the same gas flow with a ramp rate of 10 °C min^{-1} and then held at the same temperature for 20 min. Finally, the catalyst was cleaned with 8 vol.% O_2, 5 vol.% H_2O and Ar for 20 min at 500 °C before cooling down to room temperature. After pre-treatment, the fresh (non-poisoned) catalyst was transferred to another horizontal quartz tube, using the same reactor, for phosphorus poisoning experiments, as described in the next sub-section.

2.2.2. Phosphorus poisoning of monolith catalysts under NH_3-free lean hydrothermal conditions

In a typical experiment simulating phosphorus poisoning, diluted aqueous H_3PO_4 solution, which was prepared from 85% orthophosphoric acid (Merck, boiling point 158 °C), was injected into the reactor inlet with a syringe pump at a specific injection rate. We ran several preliminary tests of evaporation of the H_3PO_4 solution (2000 ppm) at different temperatures and found 200 °C was sufficient to evaporate the H_3PO_4 solution, and the reactor inlet was consequently heated up to 200 °C. A gas flow consisting of 8 vol.% O_2 and Ar with a total gas flow rate of 1200 ml min^{-1} (GHSV of 22,100 h^{-1}) was flowed through the reactor inlet to carry the vaporized H_3PO_4 into the reactor. The gas mixture used in the poisoning experiments was composed of 100 ppm H_3PO_4, 5 vol.% H_2O, 8 vol.% O_2 and Ar. All gas lines were heated to 200 °C to prevent the condensation of water and H_3PO_4. The reactor outlet was connected to a safety bottle for collecting the condensed H_3PO_4 solution before reaching the ventilation. During the poisoning experiments, another quartz reactor tube instead of the tube used in the activity measurements was used to ensure that no residual phosphorus remained in the reactor. After each poisoning experiment, the catalytic activities of the phosphorus-poisoned catalyst were measured by following the tests and pre-treatment described in Section 2.2.1.

Two series of experiments were carried out to study two key parameters of poisoning: temperature and duration. (1) The injection duration was fixed at 17 h for each experiment, and reactor temperatures of 160, 200, 250 and 400 °C, were used to investigate the effect of poisoning temperature. (2) The reactor temperature (i.e. poisoning temperature) was maintained at 250 °C, and injection durations of 8, 17, and 34 h were conducted to examine the effect of poisoning duration, giving a total phosphorus exposure of 2.6, 5.5 and 10.9 mmol, respectively. The monolith catalysts after degreening but before poisoning were denoted as 'fresh.' The poisoned monolith catalysts were denoted as 'P-Temperature-Time.' For instance, a catalyst poisoned at 250 °C for 8 h was denoted as P-250C-8h. As the two series of experiments were performed separately, there were two catalysts poisoned under the same poisoning conditions, i.e. 250 °C for 17 h, which were denoted as P-250C-17h-a and P-250C-17h-b to distinguish them in the investigations of poisoning temperature and duration, respectively. The amounts of deposited phosphorus were found to deviate between these two samples, and this can be seen in a comparison of the results from P-250C-17h-a and P-250C-17h-b in Sections 3.1 and 3.2. The reason for this deviation could be that some phosphorus remained deposited on the reactor wall even though we had carefully insulated and heated all parts and thoroughly washed the reactor tube after each poisoning.

2.2.3. Phosphorus poisoning of monolith catalysts under NH_3-SCR operating conditions

The poisoning experiments under NH_3-SCR operating conditions were performed on the same flow setup and using the same procedure as described in Section 2.2.2. The gas composition during poisoning experiments was switched to 100 ppm H_3PO_4, 400 ppm NH_3, 400 ppm NO, 5 vol.% H_2O, 8 vol.% O_2 and Ar. The poisoned monolith catalysts were denoted as 'PSCR-Temperature-Time'. For instance, a catalyst poisoned at 200 °C for 17 h under NH_3-SCR operating conditions was denoted as PSCR-200C-17h. After each poisoning experiment, the catalytic activities of phosphorus-poisoned catalyst were measured by following the tests described in Section 2.2.1.

2.2.4. Evaluation of catalyst deactivation

The degree of catalyst deactivation was evaluated by adapting the methodology described elsewhere [36]:

$$\text{Deactivation (\%)} = [1 - \left(\frac{1-X_{poisoned}}{1-X_{fresh}}\right)] \times 100\% \quad (1)$$

where $X_{poisoned}$ and X_{fresh} are the conversions of poisoned catalyst and fresh catalyst, respectively.

2.3. Catalyst characterization

It should be noted that samples used for characterization were spent catalysts, meaning that both non-poisoned and phosphorus-poisoned catalysts had already been exposed to the testing conditions described in Section 2.2.1. In this way, we could gain better understanding of phosphorus poisoning behavior under conditions similar to real world conditions. The samples were cut perpendicularly to the gas flow direction and denoted the gas-in part and gas-out part as _inlet and _outlet, respectively.

Images and elemental mappings of samples were acquired with an FEI Quanta 200 ESEM (Environmental SEM) coupled with an Oxford X-max 80 EDX detector. The elemental analysis was performed using an inductively coupled plasma sector field mass spectrometry (ICP-SFMS) by ALS Scandinavia AB. The BET surface area and pore volume were determined with an N_2 physisorption at −150 °C using a Tristar 3000 (Micromeritics) instrument. Prior to the measurement, monolith samples were degassed at 240 °C for 3 h.

H_2-TPR was conducted in a Setaram Sensys DSC (Digital Scanning Calorimeter). The H_2 concentration in the exhaust gas was monitored with a mass spectrometer (HIDEN, HPR-20 QUI). A few channels of the monolith were cut out, typically weighing about 100 mg, and were loaded in the reactor. The sample was exposed to 0.3 vol.% H_2 in Ar at a flow rate of 20 ml min^{-1} and, subsequently, heated from room temperature to 800 °C with a ramp rate of 10 °C min^{-1} and maintained for 30 min before cooling down. No pre-treatment was done prior to the TPR in order to avoid removing any phosphorus species.

X-ray photoelectron spectroscopy (XPS) measurements were performed with a PerkinElmer PHI 5000C ESCA system, which was equipped with a monochromatic Al K αX-ray source (1486.6 eV, 12 kV, 22 mA) as an incident radiation and a hemispherical energy analyzer. Charging effects were compensated using a flood gun. The base pressure in the measurement chamber was around 1×10^{-10} torr. For XPS measurement, the poisoned monolith sample was cut axially to obtain a single channel, which was then fixed on a home-made sample holder. The binding energies were calibrated using the C 1 s peak at 284.5 eV as an internal reference. For spectra deconvolution, a Shirley background, a Gaussian–Lorentzian mixed function with a ratio of 70:30, an FWHM of 1.6 eV were applied for fitting each component.

3. Results

3.1. Phosphorus poisoning of monolith catalysts under NH_3-free lean conditions

3.1.1. Variations of poisoning temperature

The surface composition of the catalyst washcoats after phosphorus poisoning was investigated using XPS. Three different locations on each sample (inlet, middle, and outlet) were measured to determine the axial distribution of phosphorus along the channel. Fig. 1 shows the normalized P 2*p* XP core-level spectra of the phosphorus-poisoned Cu-SSZ-13 samples under different poisoning temperatures. The three major contributions were attributed to phosphorus oxide (P_2O_5) at around 135.6 eV, metaphosphate (PO_3^-) at around 134.5 eV, and phosphate (PO_4^{3-}) at around 133.2 eV [43]. The spectral deconvolution showed that metaphosphate was the main compound on all phosphorus-poisoned samples. The decreasing peak area from inlet to outlet implies that the total amount of phosphorus decreases axially (Fig. 1a–d). This was further supported by the surface phosphorus contents calculated using XP survey spectra, as shown in Table 1. Similar decreasing trends in the axial distribution of phosphorus could be observed on all samples, despite differences in poisoning temperatures.

The relative concentrations of the three phosphorus compounds were calculated and are presented in Fig. 1e–h. The figure clearly shows that metaphosphate was the dominant species on all samples. Intriguingly, the relative concentrations of PO_4^{3-}, PO_3^-, and P_2O_5 varied axially and they showed two different trends that were strongly influenced by the poisoning temperature. The relative concentration of PO_4^{3-} for P-160C-17 h and P-200C-17 h increased axially (inlet → outlet), and, correspondingly, the relative concentration of P_2O_5 decreased while the relative concentration of PO_3^- changed only slightly. The variations in the relative concentrations of these three P species for P-250C-17 h-a and P-400C-17 h exhibited a trend that was the opposite of P-160C-17 h and P-200C-17 h. P_2O_5 was always more dominant than PO_4^{3-} in the three measured spots on each sample. Additionally, all the samples used in the above XPS study have experienced NH_3-related reactions, which is very close to the real application. However, for mechanistic understanding it is important to investigate the impact of NH_3-related reactions on the phosphorous oxides' (i.e., P_2O_5, PO_3^- and PO_4^{3-}) distribution. The XPS results of fresh and spent P-poisoned Cu-SSZ-13 are displayed in Fig. S1. It is interesting that NH_3-related reactions on the P-poisoned Cu-SSZ-13 seem to have a certain impact on the formation of phosphorous species. As we can observe from Fig. S1, PO_4^{3-} species are barely existing in the fresh P-poisoned Cu-SSZ-13, where the majority is PO_3^- with around 80%.

However, XPS is limited to measuring the surface of the catalyst washcoats. It has been reported that phosphorus-poisoned species not only deposit on the surface of the washcoat but also migrate into the bulk of the washcoat [17,44,45]. Therefore, it is essential to determine the total amount of phosphorus stored in the poisoned catalysts. The total P contents of the poisoned Cu-SSZ-13 monolith catalysts under different poisoning temperatures were measured using ICP-SFMS. Prior to the measurements, the poisoned monolith samples were cut perpendicularly to the monolith axial flow direction and divided into inlet and outlet parts. The results are shown in Table 2. The P contents in the inlets were always higher than the contents in the outlets of all poisoned catalysts, which was in good agreement with XPS results. The total P content in both the inlets and outlets increased with poisoning temperature from 160 °C to 250 °C and dropped somewhat at a poisoning temperature of 400 °C. The Cu contents were quite consistent in inlets and outlets, showing that the washcoating was even over the monoliths, since crushed monoliths were used for the ICP measurements. The variation of P content on the different poisoned catalysts yielded variation on the P/Cu ratio. A higher P/Cu ratio indicated a higher possibility that phosphorus species had interacted with Cu ions in the zeolite pores [41].

The H_2-TPR experiments were performed using smaller pieces (2 × 2 channels) of monolith catalysts, which were cut from the inlet and outlet of original monolith catalysts. The TPR profiles of the fresh and phosphorus-poisoned Cu-SSZ-13 at different poisoning temperatures are shown in Fig. 2. The inlet and outlet of fresh catalyst both show similar broad peaks of hydrogen consumption centered at around 300 °C. After phosphorus poisoning, the peak temperatures of the main hydrogen consumption of all the phosphorus-poisoned catalysts shifted to around 500 °C, indicating changes in Cu coordination inside zeolite pores due to copper-phosphorus interaction [41]. The degree of shift in temperature was connected to the poisoning temperature. For example, the peak reduction temperature shifted to 450 °C, 470 °C, and 500 °C for the samples poisoned at 160 °C, 200 °C, and 250 °C, respectively. While the temperature shifted down to 490 °C for the sample poisoned at 400 °C. It was also found that the peak reduction temperature of the inlet parts always shifted to higher temperatures than the corresponding outlet parts.

The influence of phosphorus poisoning on Cu-SSZ-13 activity was mainly evaluated with a standard NH_3-SCR reaction (Eq. 2). NH_3 oxidation (Eq. 3) and NO oxidation (Eq. 4) were implemented to probe the

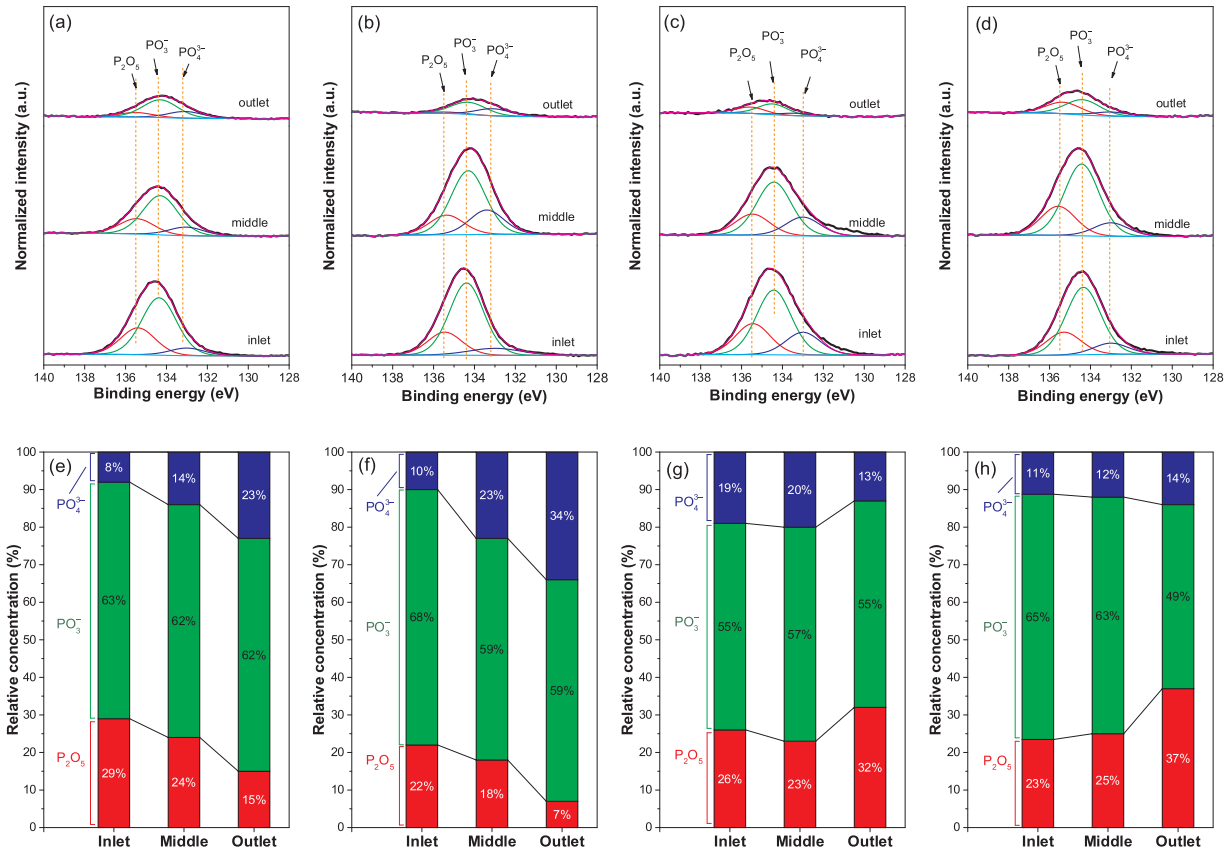

Fig. 1. XP P 2*p* spectra of the Cu-SSZ-13 samples poisoned at different poisoning temperatures. The spectra were normalized to the intensity of the corresponding O 1 s spectra. Relative concentrations of the phosphorus species obtained with the deconvolution of the corresponding XP P 2*p* spectra. (a, e) P-160C-17h, (b, f) P-200C-17h, (c, g) P-250C-17h-a, (d, h) P-400C-17h.

Table 1
Atomic concentration of surface P on the Cu-SSZ-13 monolith samples poisoned at different temperatures.

Samples	Surface P content (atomic%)		
	Inlet	Middle	Outlet
P-160C-17h	7.9	4.8	2.8
P-200C-17h	9.4	7.4	2.5
P-250C-17h-a	9.0	6.9	2.9
P-400C-17h	6.9	7.9	2.7

influence of phosphorus on the copper sites where NH_3 oxidation and NO oxidation reactions occur. The storage and release of ammonia in the zeolite catalysts are believed to play crucial roles in SCR reactions and strongly affect the catalyst's efficiency of NO_x abatement, especially during transient operations [46–48]. Therefore, studying ammonia oxidation, NO oxidation, and ammonia storage over the catalysts before and after poisoning will give supplementary understanding of the phosphorus poisoning effect on Cu-SSZ-13 as SCR catalysts. Moreover, NO storage experiments were also conducted to examine if the NO-Cu interactions had changed due to poisoning. It is necessary to recall that the catalytic activity of each monolith catalyst was always evaluated before and after phosphorus poisoning on the same monolith to ensure that the observed differences were indeed due to phosphorus poisoning.

$$4NO + 4NH_3 + O_2 \rightarrow 4N_2 + 6H_2O \quad (2)$$

$$4NH_3 + 3O_2 \rightarrow 2N_2 + 6H_2O \quad (3)$$

$$2NO + O_2 \leftrightarrow 2NO_2 \quad (4)$$

Fig. S2a–d (supplementary material) shows the NH_3 storage-desorption profiles for the Cu-SSZ-13 catalysts before and after poisoning at different temperatures. In the adsorption phase, the time of NH_3 uptake on the poisoned catalysts was slightly shorter than the fresh counterparts. In the desorption phase, three types of acidic sites were identified according to the assignment described in our previous work [13]. The three peaks at low temperature (˜ 230 °C), intermediate temperature (˜ 330 °C), and high temperature (˜ 435 °C) corresponded to the loosely bound NH_3 on week acidic sites (S3), moderately bound NH_3 on stronger acidic sites (S1), and strongly bound NH_3 on the strongest

Table 2
P and Cu contents and P/Cu ratio of the Cu-SSZ-13 monolith samples poisoned at different temperatures.

Samples	P content (wt.%)			Cu content (wt.%)			P/Cu ratio		
	Inlet	Outlet	Mean	Inlet	Outlet	Mean	Inlet	Outlet	Mean
P-160C-17h	0.17	0.04	0.10	0.90	0.88	0.90	0.39	0.09	0.23
P-200C-17h	0.35	0.06	0.20	0.93	0.90	0.91	0.77	0.14	0.45
P-250C-17h-a	0.56	0.19	0.39	0.93	0.94	0.93	1.23	0.41	0.86
P-400C-17h	0.41	0.17	0.29	0.92	1.02	0.97	0.91	0.34	0.61

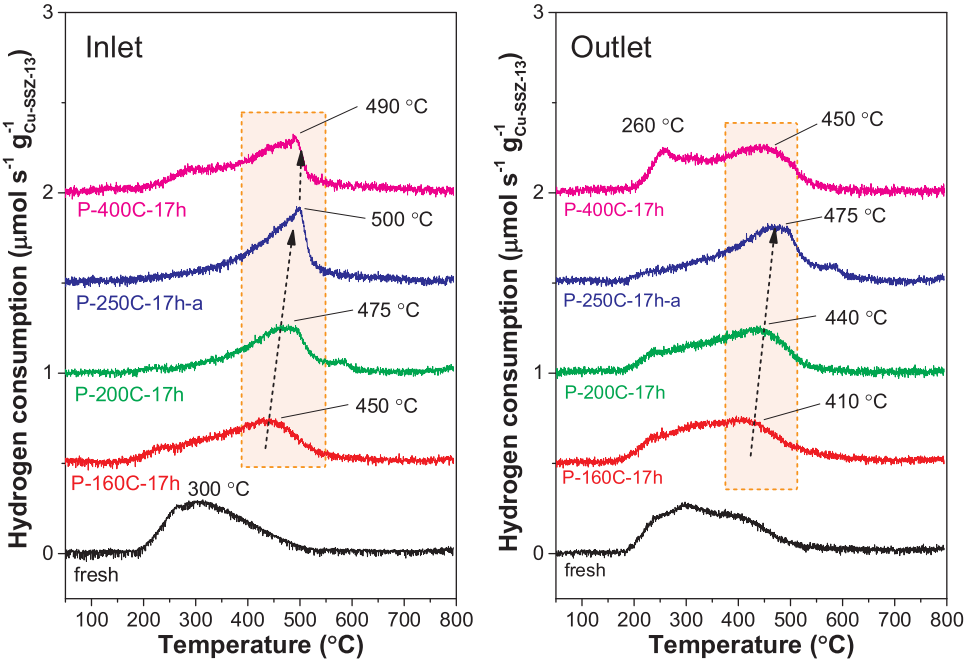

Fig. 2. H_2-TPR profiles of fresh and phosphorus-poisoned Cu-SSZ-13 samples at different poisoning temperatures. Left: inlet; right: outlet.

acidic sites (S2), respectively. The phosphorus-poisoned catalysts, P-200C-17h, P-250C-17h-a and P-400C-17h, exhibited a decrease in NH_3 storage while P-160C-17h showed unchanged NH_3 storage. The decrease in NH_3 storage was mainly found on the S1 sites, although the decrease was small. Furthermore, the individual NH_3 storage on each acidic site and the total NH_3 storage were determined by using a three-peak fitting method (Fig. S3), which was adapted from our previous work [49]. The results summarized in Fig. S2e show that the phosphorus poisoning mainly lowered the NH_3 storage on S1 and S3 sites, but barely impacted the S2 site. However, the impact of phosphorus poisoning on NH_3 storage was minor.

The results of NO-TPD are displayed in Fig. S4. The NO-TPD experiments were conducted in the absence of water due to the blocking effect of water. The adsorption of NO was found to be on Cu^{2+} sites with the use of IR spectroscopy [50,51]. Quantifications of total NH_3 storages and NO storages for fresh and poisoned Cu-SSZ-13 catalysts are compared in Table S1. The poisoning effect of phosphorus on NO storage was found to be very similar to the NH_3-TPD experiments. The P-250C-17h-a sample showed the greatest losses of the total NH_3 storage and NO storage among the poisoned catalysts. Moreover, from the data in Table S1, it is clear that the NO/Cu ratio always is lower than 1, ranging from 0.7 for fresh catalyst to 0.2 for the most deactivated sample, suggesting that NO is adsorbed on the copper sites. However, the ammonia storage is much larger, ranging from 1.7 for the most deactivated sample to 2.3 for fresh sample. These results are reasonable since it is well known that multiple ammonia can adsorb on one copper and also that ammonia is stored on Brönsted acid sites as well.

Fig. 3 shows the performance of NH_3 oxidation for the Cu-SSZ-13 monolith catalysts before and after poisoning at different temperatures. Only low concentrations of N_2O (< 3 ppm, see Fig. S5) were detected in the exhaust, and the formation of NO or NO_2 was not observed using an MKS FT-IR analyzer, indicating that ammonia oxidation mainly produced N_2. Detailed explanations of the catalytic behavior of NH_3 oxidation and N_2O formation have been reported in our previous study [39]. The results in Fig. 3 show a clear poisoning effect on ammonia oxidation activity for all poisoned catalysts. Correspondingly, the formation of N_2O was suppressed (Fig. S5). The poisoning effect was also probed for the performance of the NO oxidation of the Cu-SSZ-13 monolith catalysts before and after poisoning at different temperatures, as presented in Fig. S6. The similar poisoning effect trend for both NH_3 oxidation and NO oxidation demonstrates that the loss of oxidation activity caused by phosphorus is temperature-dependent. However, the differences in deactivation between P-250C-17h and P-400C-17h were minor.

Fig. 4 shows the steady-state values of NO_x conversions of standard NH_3-SCR for the Cu-SSZ-13 monolith catalysts before and after poisoning at different temperatures. Both fresh and phosphorus-poisoned catalysts were almost inactive when reaction temperatures were below 100 °C, and they became active for NO_x reduction at higher reaction temperatures. The NO_x conversions of fresh catalysts increased from 0% to nearly 100% by increasing reaction temperatures from 100 °C to 200 °C. The NO_x conversions maintained at 100% between 200–300 °C, and then dropped to nearly 90% when the reaction temperatures were increased up to 500 °C. The influence of phosphorus poisoning on NO_x reduction over P-160C-17h was almost negligible, despite the existence of some phosphorus (0.11 wt.%). This was consistent with the observations made for NH_3-TPD (Fig. 2), NO-TPD (Fig. S4), NH_3 oxidation (Fig. 3), and NO oxidation reactions (Fig. S6), where the impact of phosphorus poisoning on P-160C-17h was minor. With a reaction temperature of 200 °C or lower, a minor deactivation occurred on P-200C-17h and became more significant on P-250C-17h-a, while the deactivation was reduced for P-400C-17h. Phosphorus-poisoned catalysts showed minor improvements in NO_x conversion at a reaction temperature higher than 300 °C, which can be attributed to the phosphorus inhibition of NH_3 oxidation [39]. The formation of N_2O during standard NH_3-SCR for the Cu-SSZ-13 monolith catalysts before and after poisoning was also monitored, and steady-state values are shown in Fig. S7. Detailed explanations for the N_2O formation during standard SCR have been reported in our previous study [39]. The N_2O formation was inhibited for all poisoned catalysts. The inhibition effect correlated with the poisoning temperature. The concentrations of N_2O produced in standard NH_3-SCR were noted to be higher than those generated in NH_3 oxidation (Fig. S5).

3.1.2. *Variations of poisoning duration*

In another series, the poisoning duration was varied and the poisoning temperature was fixed at 250 °C, based on the results from variations of poisoning temperature, where the Cu-SSZ-13 catalyst

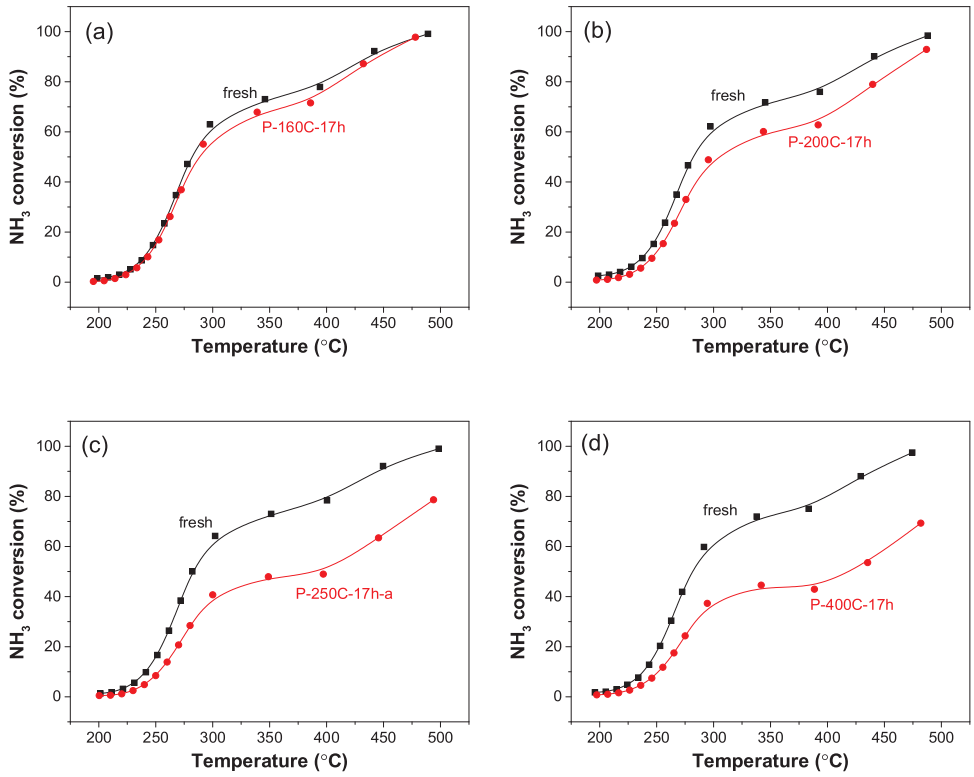

Fig. 3. NH_3 conversion as a function of temperature during NH_3 oxidation over the Cu-SSZ-13 catalysts before and after poisoning at different temperatures: (a) 160 °C, (b) 200 °C, (c) 250 °C, (d) 400 °C. Reaction conditions: 400 ppm NH_3, 8 vol.% O_2, 5 vol.% H_2O and Ar at 22,100 h^{-1}.

exposed to 100 ppm H_3PO_4 at 250 °C for 17 h was the most deactivated.

Table 3 summarizes the phosphorus and copper contents in inlet and outlet parts of the Cu-SSZ-13 monolith catalysts poisoned at different durations. As expected, the results showed that all poisoned catalysts contained higher phosphorus contents in the inlet parts than in the outlet parts. Prolongation of poisoning duration led to greater P content and increased the P/Cu ratio in both inlet and outlet parts for all poisoned catalysts. It should be noted that the capturing efficiency (moles P in monolith determined by ICP divided by total moles of P during exposure) is only 1–2%. This means that most of the phosphorus

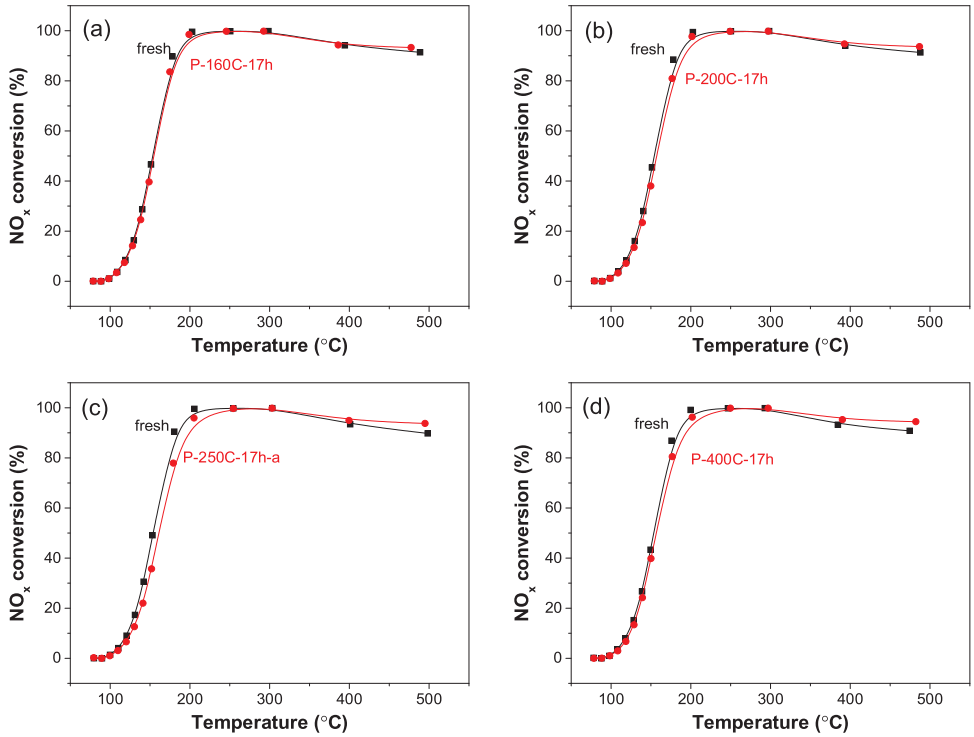

Fig. 4. NO_x conversion as a function of temperature during standard NH_3-SCR over the Cu-SSZ-13 catalysts before and after poisoning at different temperatures: (a) 160 °C, (b) 200 °C, (c) 250 °C, (d) 400 °C. Reaction conditions: 400 ppm NH_3, 400 ppm NO, 8 vol.% O_2, 5 vol.% H_2O and Ar at 22,100 h^{-1}.

Table 3
P and Cu contents and P/Cu ratio on the Cu-SSZ-13 monolith samples poisoned for different durations.

Samples	P content (wt.%)			Cu content (wt.%)			P/Cu ratio		
	Inlet	Outlet	Mean	Inlet	Outlet	Mean	Inlet	Outlet	Mean
P-250C-8h	0.61	0.19	0.40	0.97	1.02	0.99	1.29	0.38	0.83
P-250C-17h-b	0.88	0.54	0.72	0.91	1.08	0.99	1.98	1.02	1.49
P-250C-34h	1.19	0.66	0.90	1.03	0.91	0.96	2.37	1.49	1.92

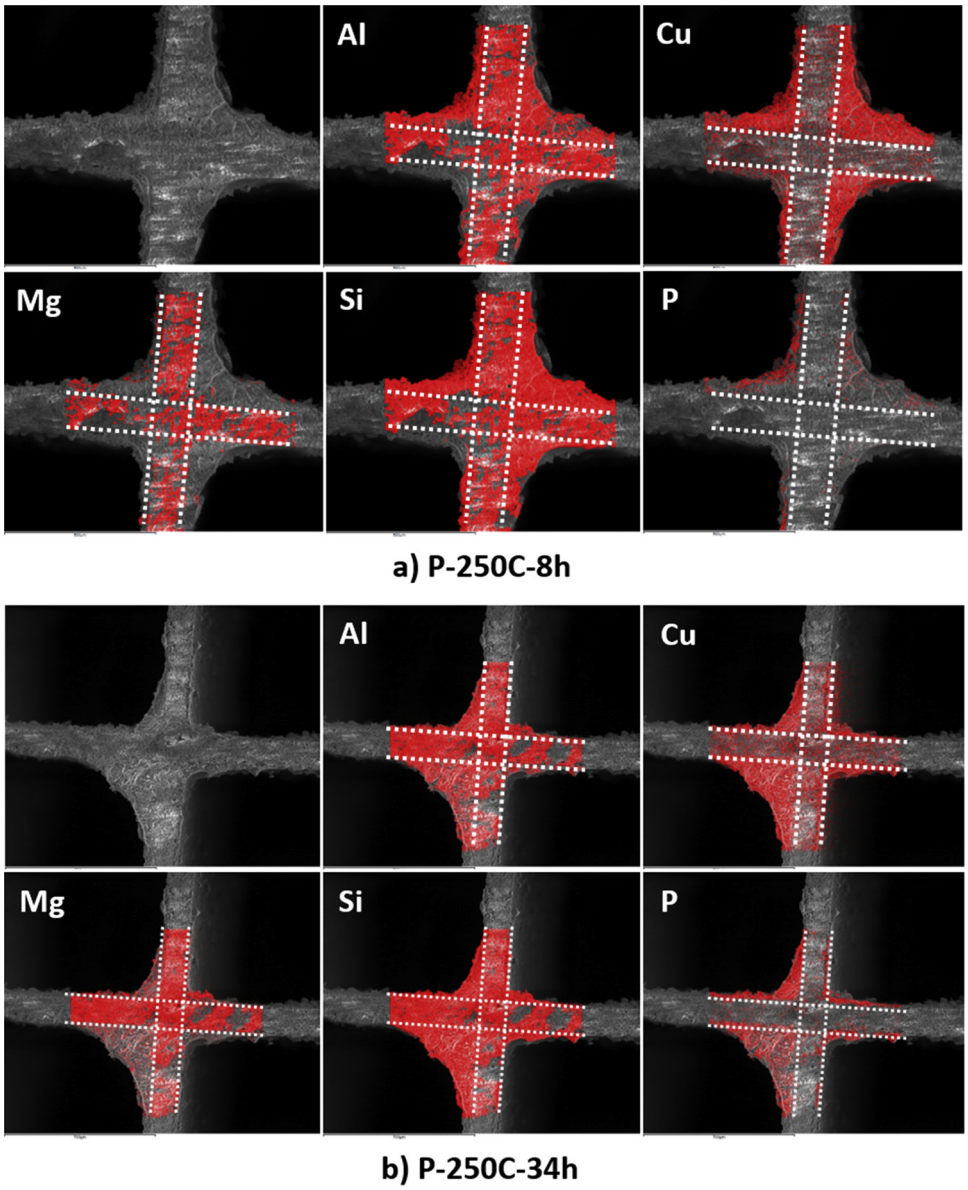

Fig. 5. Representative SEM-EDX element mappings of the inlets of (a) P-250C-8h and (b) P-250C-34h.

passes through the catalyst and indeed acid water was captured after the reactor during the experiments. The 34 h long experiment resulted in about two times as much P, according to ICP, compared to the 8 h experiment. This shows that the catalyst was not saturated after 8 h even though the capturing efficiency was low, but instead that the phosphorus poisoning is a slow process with a low reaction rate.

EDX elemental mapping under SEM observation was performed to examine the radial distributions of Mg, Al, Si, Cu, and P elements on the inlet parts of Phosphorus-poisoned Cu-SSZ-13 monolith catalysts, as shown in Fig. 5. Prior to the measurement, about 1–3 mm of the immediate front of inlet parts was removed to expose the cross-sectional surface of the monoliths. It should be noted that the Al and Si elements in the mappings were derived from both cordierite and catalyst washcoat, while the Mg element in the mappings was solely from cordierite. The Cu mappings suggest that Cu was well distributed in the washcoat layer. The P mappings of the P-250C-8h sample displayed a P-rich phase on the surface/subsurface of the washcoat and a P-deficient phase in the bulk of the washcoat, as presented in Fig. 5a. However, the P mappings of the P-250C-34h sample showed a more homogeneous dispersion of phosphorus in the surface and bulk of the washcoat (Fig. 5b). On the one hand, our results are in line with the observations reported in previous studies [17,44,52], where P species were found to

preferentially deposit on the inlet and surface of catalysts. On the other hand, our results have also demonstrated that the deposition of P species in the washcoat involves a diffusion process in which the P species is first accumulated on the surface/subsurface with a short poisoning duration, and then diffused through the bulk of washcoat layer with a prolonged poisoning duration. Our results are in good agreement with the phosphorus poisoning model for a diesel oxidation catalyst developed by Nagata and Tanaka [45]. Those authors found that the P species was first anchored on the washcoat surface and then migrated into the bulk by means of solid diffusion.

Fig. S8 shows a comparison of H_2 consumption profiles during H_2-TPR from Phosphorus-poisoned Cu-SSZ-13 monolith samples with a fresh Cu-SSZ-13 monolith sample. Significant changes in peak reduction temperatures were observed for all poisoned catalysts, indicating that there was a major interaction of copper-phosphorus. The shift in peak reduction to higher temperatures was found to correlate with poisoning duration, and the same trends were observed for the samples from both inlet and outlet parts. It should be noted that the peak reduction temperature always shifted to a higher temperature on inlet samples than on outlet samples.

Fig. 6a–c shows the NH_3 storage-desorption profiles for the Cu-SSZ-13 catalysts before and after poisoning at different durations. A decrease in NH_3 storage for all poisoned catalysts was directly indicated by the shorter NH_3 uptake time during the adsorption phase and a lower concentration of NH_3 during the desorption phase. The NH_3 storage of individual sites and the total NH_3 storage were obtained using three-peak fitting [49]. The results are shown in Fig. S9 and Fig. 6d. The NH_3 storage of S1 and S3 and the total NH_3 storage decreased with an increase in poisoning duration from 8 h to 34 h, while the NH_3 storage on S2 (peak at the highest temperature) showed enhancements after poisoning. Fig. S10 shows the NO storage-desorption profiles for Cu-SSZ-13 catalysts before and after poisoning at different durations. A detrimental effect of phosphorus was found for NO storage as evidenced by the dramatic decline in NO uptakes and desorption peak intensities of poisoned catalysts. Quantifications of total NH_3 storages and NO storages for fresh and poisoned Cu-SSZ-13 catalysts are compared in Table S1.

Fig. 7 and Fig. S11 show steady-state NH_3 conversion and N_2O concentrations during NH_3 oxidation for the Cu-SSZ-13 monolith catalysts before and after poisoning at different durations. All phosphorus-poisoned catalysts showed remarkable decrease in NH_3 conversions comparing to the corresponding fresh catalysts, demonstrating that the copper sites used for NH_3 oxidation on Cu-SSZ-13 catalysts were severely poisoned by phosphorus. The degree of deactivation was correlated to the poisoning duration. Moreover, N_2O formation was also significantly inhibited on the phosphorus-poisoned catalysts. A similar poisoning-duration dependent effect were observed on NO oxidation performances for the Cu-SSZ-13 monolith catalysts after poisoned at different durations (Fig. S12). In particular, the catalyst exposed to 100 ppm H_3PO_4 at 250 °C for 34 h (P-250C-34h) exhibited drastic losses of activities during NH_3 oxidation and NO oxidation reactions, likely due to the large P content.

Fig. 8 shows a comparison of the performance of standard SCR reactions for the Cu-SSZ-13 monolith catalysts before and after poisoning at different durations. The formation of N_2O during SCR for the corresponding catalysts is shown in Fig. S13. At reaction temperatures of 300 °C or below, the poisoned catalysts showed a decrease in the NO_x conversion as the poisoning temperature increased. While at reaction temperatures of 400 °C or above, NO_x conversion was enhanced to a slightly larger extent for P-250C-8h and to a smaller extent for P-250C-17h-b, which can be attributed to the suppressed NH_3 oxidation caused by phosphorus poisoning, as demonstrated in the results for NH_3 oxidation (Fig. 7). However, when the poisoning duration was as long as 34 h, P-250C-34h exhibited a decline in the NO_x conversion at reaction temperatures of 400 °C or above, indicating that phosphorus deactivated the copper sites for NH_3-SCR at high reaction temperatures.

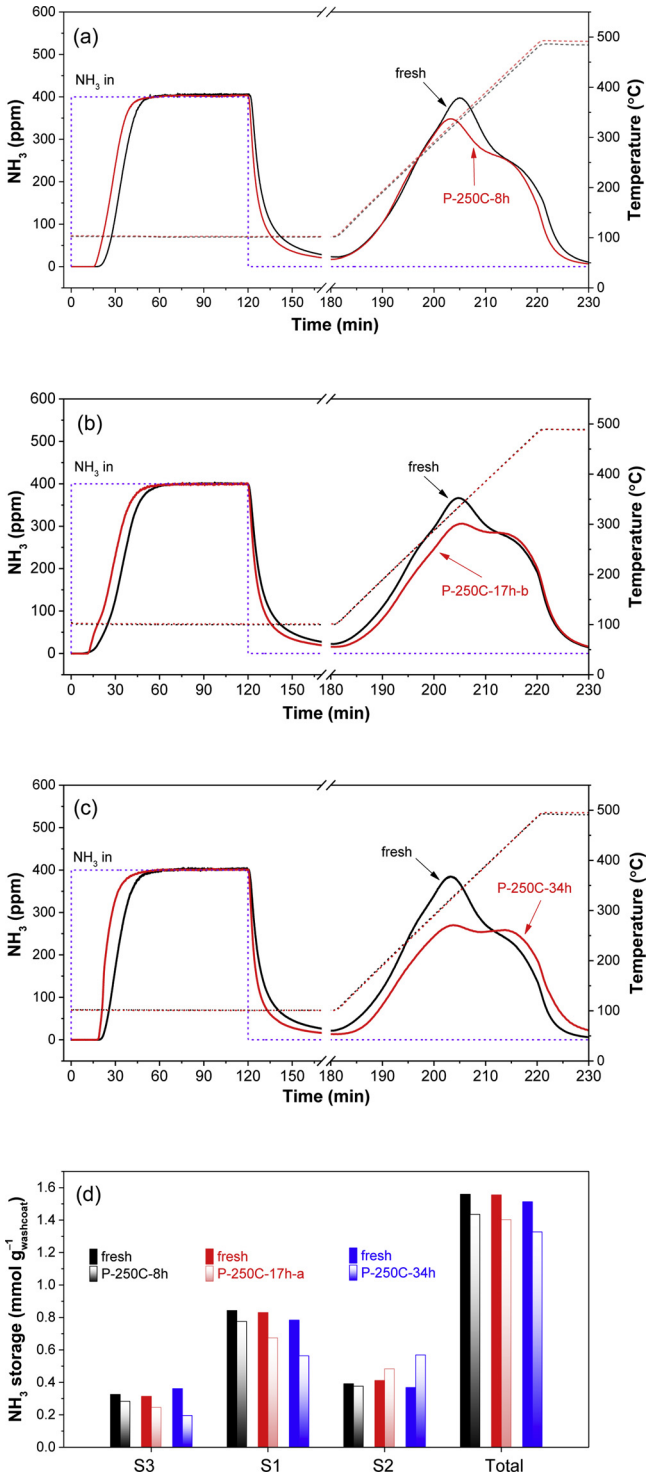

Fig. 6. NH_3-TPD profiles for the Cu-SSZ-13 catalysts before and after poisoning for different durations: (a) 8 h, (b) 17 h, and (c) 34 h. The catalysts were exposed to 400 ppm NH_3, 5 vol.% H_2O and Ar for 120 min at 100 °C followed by purging with Ar for 60 min. Ramp: 10 °C min^{-1}. (d) Estimated individual NH_3 storage on S3, S1, and S2 and total NH_3 storage for the corresponding catalysts.

3.2. Phosphorus poisoning under NH_3-SCR operating conditions

In this section, the study of the effect of H_3PO_4 poisoning in the presence of NH_3, NO, O_2, and H_2O at different temperatures (i.e. 200, 250, and 400 °C) is investigated. The aim was to replicate phosphorus poisoning under real NH_3-SCR operating conditions. Briefly, the catalysts were exposed to 100 ppm H_3PO_4 for 17 h in the presence of

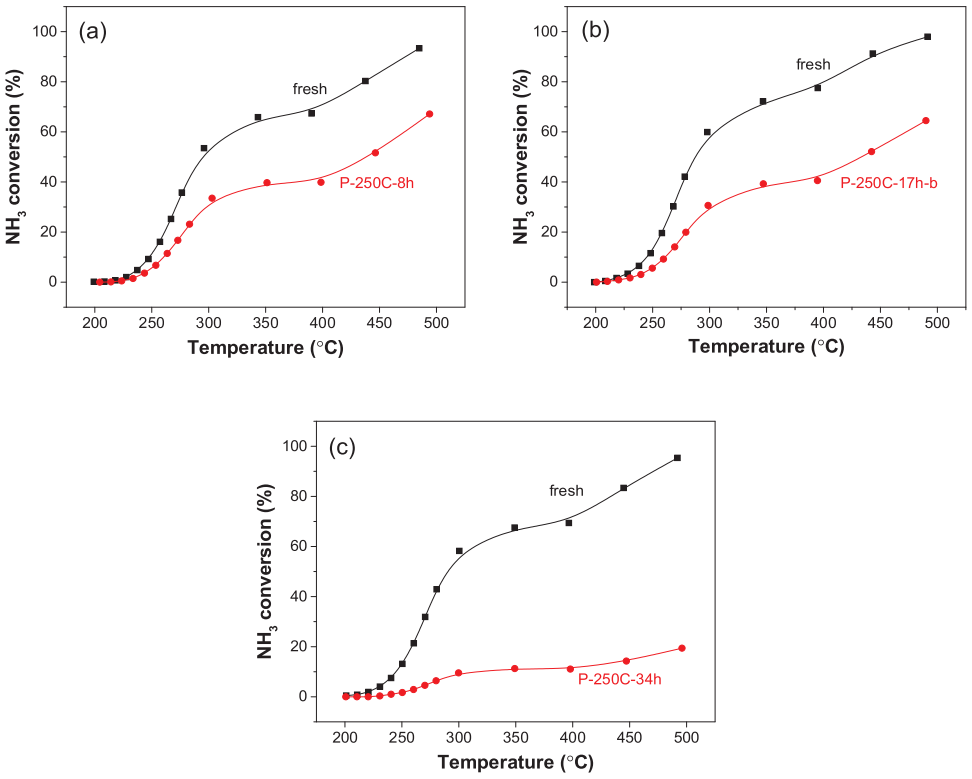

Fig. 7. NH_3 conversion as a function of temperature during NH_3 oxidation over the Cu-SSZ-13 catalysts before and after poisoning for different durations: (a) 8 h, (b) 17 h, and (c) 34 h. Reaction conditions: 400 ppm NH_3, 8 vol.% O_2, 5 vol.% H_2O and Ar at 22,100 h^{-1}.

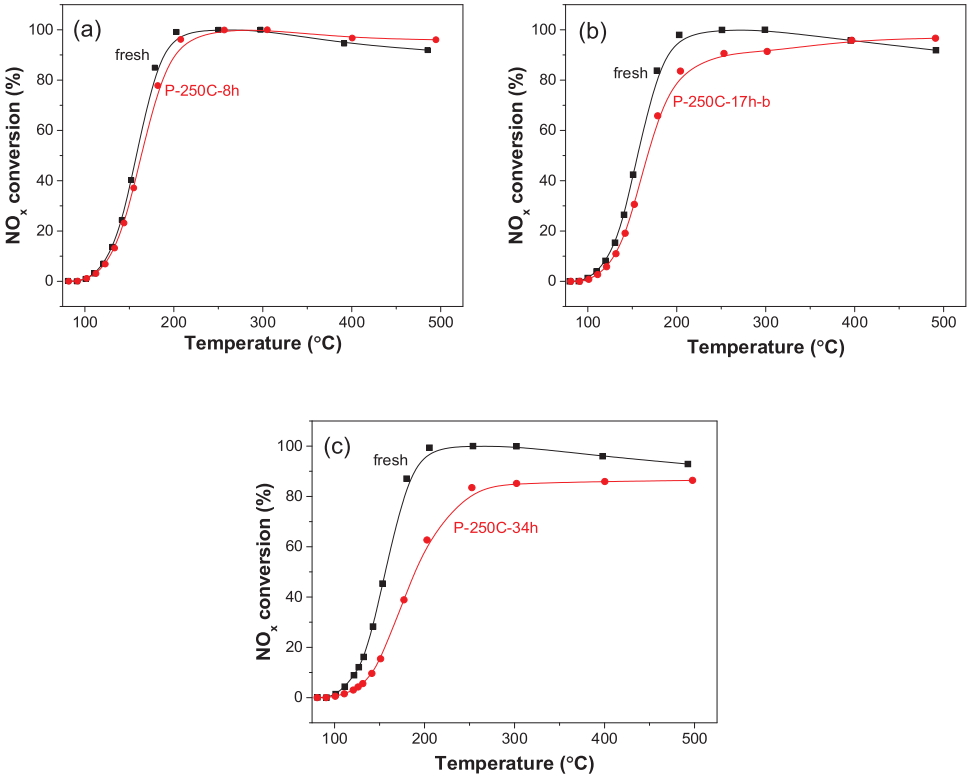

Fig. 8. NO_x conversion as a function of temperature during standard NH_3-SCR over the Cu-SSZ-13 catalysts before and after poisoning for different durations: (a) 8 h, (b) 17 h, and (c) 34 h. Reaction conditions: 400 ppm NH_3, 400 ppm NO, 8 vol.% O_2, 5 vol.% H_2O, and Ar at 22,100 h^{-1}.

Table 4
P and Cu contents and P/Cu ratio for the Cu-SSZ-13 monolith samples poisoned at different NH_3-SCR operating temperatures.

Samples	P content (wt.%)			Cu content (wt.%)			P/Cu ratio		
	Inlet	Outlet	Mean	Inlet	Outlet	Mean	Inlet	Outlet	Mean
PSCR-200C-17h	0.06	0.02	0.03	0.97	0.96	0.96	0.13	0.02	0.06
PSCR-250C-17h	0.14	0.09	0.11	1.11	1.11	1.11	0.26	0.17	0.20
PSCR-400C-17h	0.33	0.14	0.24	1.15	1.02	1.08	0.59	0.28	0.46

400 ppm NH_3, 400 ppm NO, 5 vol.% H_2O, 8 vol.% O_2 at 200, 250, and 400 °C, respectively. After each poisoning experiment, a deposit of white particles was visible on the reactor wall owing to the formation of ammonia phosphate particles. Even though we injected the phosphorus acid directly into the heated reactor with a Teflon line, these deposits could not be avoided. However, when the temperature was increased, the amount of deposits decreased. These results have a practical implication because there will likely be deposits in the aftertreatment system if phosphorus and ammonia co-exist at low to medium temperatures.

The P and Cu contents measured using ICP-SFMS are presented in Table 4. As expected, the P content shows an axial distribution over each poisoned catalyst in the table, i.e. a higher content of P in the inlet samples and a lower content of P in the outlet samples. A comparison of the P content on the samples poisoned without the presence of NH_3 under same poisoning temperatures (Table 2) showed that the P contents on the samples poisoned under NH_3-SCR operating conditions were substantially lower. This difference can be attributed to the formation of ammonium phosphates on the reactor wall prior to the location of the catalyst, which led to less deposition of P species on the monolith samples. The P content was increased by raising the NH_3-SCR operating temperatures, which was consistent with the observation of fewer white deposits on the reactor wall. The H_2-TPR profiles of Cu-SSZ-13 samples poisoned at different NH_3-SCR operating temperatures are presented in Fig. 9. The reduction temperature again showed a shift to higher temperature for the samples poisoned at NH_3-SCR operating conditions.

Fig. S14 shows the NH_3 storage-desorption profiles for a sample before and after phosphorus poisoning under NH_3-SCR operating conditions. No change in the NH_3 storage was observed for the PSCR-200C-17h sample. The change in NH_3 storage was very little for the PSCR-250C-17h sample and became more visible on the PSCR-400C-17h sample. The NH_3 storage at an individual site and the total NH_3 storage were obtained using three-peak fitting and integration [49]. The results are shown in Fig. S15 and Fig. 9d.

As depicted in Fig. 10, the NH_3 oxidation did not change after poisoning under an NH_3-SCR operating temperature at 200 °C (PSCR-200C-17h). The oxidation became less active after poisoning under NH_3-SCR operating conditions at 250 °C (PSCR-200C-17h) and 400 °C (PSCR-400C-17h). The loss in activity became greater at higher poisoning temperatures, which is in line with the amount of P in the ICP-SFMS measurements (Table 4). The formation of N_2O (Fig. S16) was inhibited by P. The results of NO oxidation are displayed in Fig. S17, and the figure shows that the NO oxidation reaction was poisoned in a way similar to the NH_3 oxidation reaction.

The results for SCR performance over fresh and phosphorus-poisoned Cu-SSZ-13 under NH_3-SCR operating conditions are shown in Fig. 11. With the reaction temperatures below 300 °C, no deactivation in NO_x reduction can be seen on the catalyst poisoning under NH_3-SCR operating conditions at 200 °C (PSCR-200C-17h). NO_x reduction activity decreased slightly when the poisoning temperature was set to 250 °C (PSCR-250C-17h) and 400 °C (PSCR-400C-17h), and the loss of activity was greater at the higher poisoning temperature. It can be noted that the losses in the activity of the catalyst poisoned under NH_3-SCR operating conditions were smaller than the losses in the activity of the catalysts poisoned at the same temperatures but without the

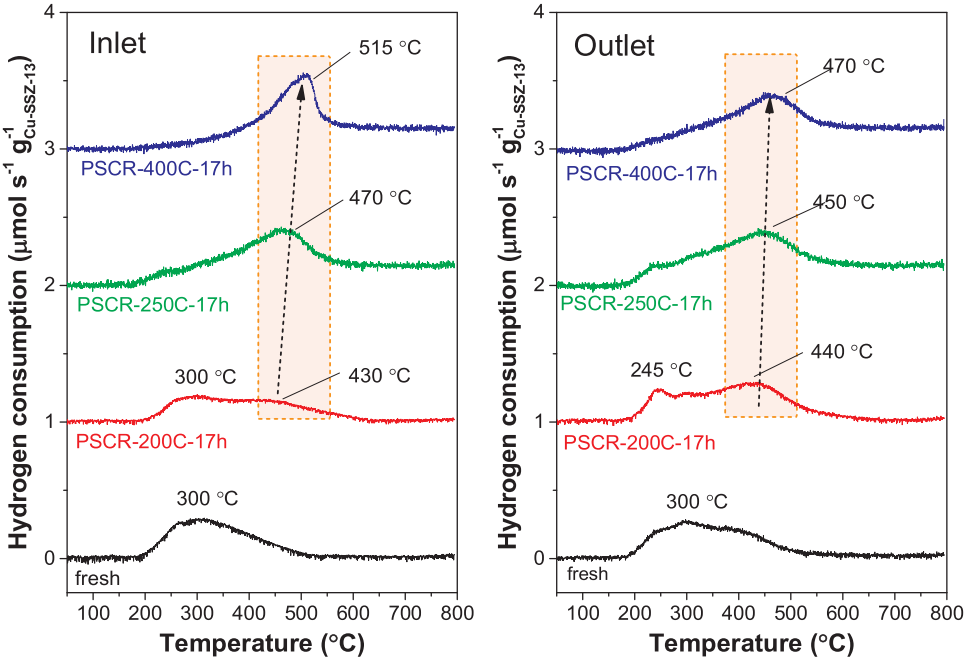

Fig. 9. H_2 consumption profiles during H_2-TPR for fresh and phosphorus-poisoned Cu-SSZ-13 monolith samples at different NH_3-SCR operating temperatures. Left: inlet; right: outlet.

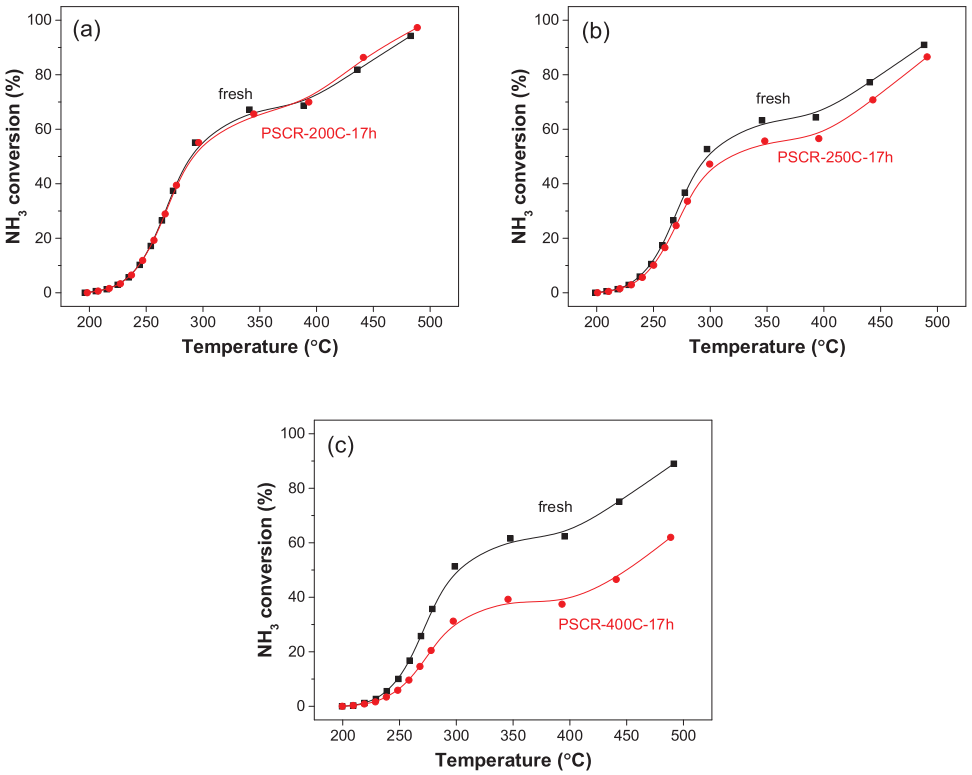

Fig. 10. NH_3 conversion as a function of temperature during NH_3 oxidation over the Cu-SSZ-13 before and after poisoning at different NH_3-SCR operating temperatures: (a) 200 °C, (b) 250 °C, and (c) 400 °C. Reaction conditions: 400 ppm NH_3, 8 vol.% O_2, 5 vol.% H_2O and Ar at 22,100 h^{-1}.

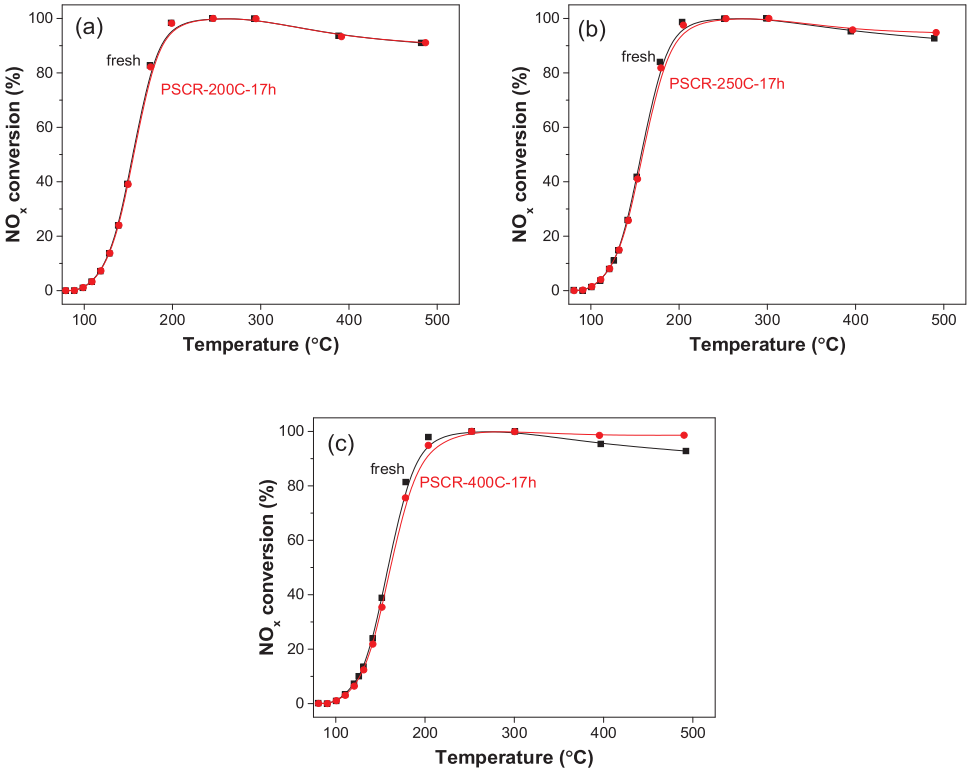

Fig. 11. NO_x conversion as a function of temperature during standard NH_3-SCR over the Cu-SSZ-13 catalysts before and after poisoning at different NH_3-SCR operating temperatures: (a) 200 °C, (b) 250 °C, and (c) 400 °C. Reaction conditions: 400 ppm NH_3, 400 ppm NO, 8 vol.% O_2, 5 vol.% H_2O and Ar at 22,100 h^{-1}.

presence of NH_3 and NO (Fig.4). This is likely due to the formation of ammonium phosphate on the reactor wall. At reaction temperatures above 300 °C, a slight improvement in NO_x reduction occurred on PSCR-250C-17h, and significantly enhanced NO_x reduction activity was found for PSCR-400C-17h at this temperature. Moreover, the formation of N_2O also inhibited phosphorus poisoning, and the degree of inhibition was greater at a higher poisoning temperature (Fig. S18).

4. Discussion

The main objective of this study was to elucidate the behavior of phosphorus poisoning of Cu-SSZ-13 catalysts under different conditions and to correlate P/Cu ratios to the reactions relevant for the selective catalytic reduction of NO (i.e. NH_3 storage and release, NO storage and release, ammonia oxidation (Eq. 2), NO oxidation (Eq. 3) and standard SCR (Eq. 1)) over phosphorus-poisoned Cu-SSZ-13.

4.1. Influence of poisoning conditions on the capture of phosphorus on a monolith

Metaphosphate was identified with XPS study as the dominant compound of the three phosphorus species on all P-poisoned samples, despite poisoning conditions and catalyst's history (i.e. whether the catalysts were exposure to NH_3-related reactions or not). This is consistent with findings in previous studies [29,42,52], where metaphosphates were also found to be the dominant specie on Cu/BEA, Fe/BEA, and Pt/Ba/Al_2O_3 catalysts poisoned with vapor-phase H_3PO_4.

The ICP results showed an axial gradient of P content on all of the poisoned catalysts that captured higher amounts of phosphorus in the inlet than in the outlet, which is in good agreement with XPS results. This finding is also consistent with other studies in the literature [16,53], where the axial gradient of the phosphorus content from the inlet to the outlet of the channels of monoliths was observed. As the evaporation temperature of H_3PO_4 solution was 158 °C, poisoning at 200 °C led to better evaporation of H_3PO_4 and less condensation of H_3PO_4 on the reactor wall than at 160 °C. This resulted in greater amounts of P captured on P-200C-17h than on P-160C-17h. The evaporation of H_3PO_4 was maximized by increasing the poisoning temperature to 250 °C. However, simultaneously, H_3PO_4 (orthophosphoric acid) started to dehydrate and form polyphosphoric acids (e.g. pyrophosphoric acid ($H_4P_2O_7$) and tripolyphosphoric acid ($H_5P_3O_{10}$)) and metaphosphoric acids (e.g. trimetaphosphoric acid ($H_3P_3O_9$)), the structures of which are usually chain-like and the boiling points are higher than for H_3PO_4 (158 °C) [53,54]. The dehydration effect became stronger at higher poisoning temperatures [53]. Therefore, poisoning at 400 °C resulted in more P deposited on the reactor wall and less P captured on the catalyst placed in the downstream position. Overall, the poisoning at 250 °C led to the Cu-SSZ-13 monolith capturing the maximum amount of P. By extending the poisoning duration (e.g. 34 h), a large amount of P could be captured on the Cu-SSZ-13 catalyst, and its SCR performance was significantly inhibited. When phosphorus poisoning was implemented under NH_3-SCR operating conditions, H_3PO_4 vapor reacted with NH_3 to form ammonia phosphates. These phosphates were deposited in the evaporation area and along the reactor wall, resulting in a small amount of P being captured on the monolith placed downstream. An increase in the poisoning temperature (i.e. reactor temperature) from 200 °C to 400 °C reduced the formation of ammonium phosphate and allowed more P to be captured on the monoliths. Interestingly, NH_3-SCR operating conditions can actually inhibit the accumulation of P on SCR catalysts, which leads to less significant deactivation. However, SCR catalysts must periodically be regenerated from sulfur at high temperatures (500 ~ 600 °C), which can decompose the ammonium phosphates and lead to the accumulation of P in a long-term application.

The deactivation mechanism caused by phosphorus poisoning is summarized in the literature in two categories: physical deactivation and chemical deactivation. (1) Physical deactivation includes the masking of a catalyst surface and blocking catalyst pores with a deposit of P [16,55,56], which hinders the access of reactant gases to active sites (i.e. reduces the number of active sites). However, we did not observe any clear drop in the BET surface area on the phosphorus-poisoned catalysts (see Table S2), and this could possibly be due to the relatively low P contents on the catalysts. (2) Chemical deactivation involves interaction between P species and catalyst components (e.g. active sites or support). For example, the formation of copper phosphates in Cu-zeolite catalysts has been found to be the main compound that causes the deactivated catalysts in NH_3-SCR [29,39]. In contrast, the formation of zinc, calcium, magnesium, aluminum, or Ce phosphates has commonly been reported for phosphorus-poisoned automotive catalysts [16,57]. For instance, aluminum phosphate has been found to be the main cause for the deactivation of three-way catalysts [57]. However, it is difficult to distinguish between the effects of physical deactivation and chemical deactivation. Physical pore blocking is unavoidable with a high level of phosphorus poisoning. In our previous work [41], we used $(NH_4)_2HPO_4$ as a poison precursor for simulating phosphorus poisoning on Cu-SSZ-13 powder catalysts and precisely controlled the P content in powder samples in the range of 0.26 ~ 1.21 wt.%. The pore-blocking effect was minor and the phosphorus poisoning had a negligible effect on the SCR performance, but, interestingly, the poisoning had detrimental impacts on ammonia and NO oxidation [41].

To the best of our knowledge, no study has reported gas-phase phosphorus poisoning of Cu-SSZ-13 under either NH_3-free lean conditions or NH_3-SCR operating conditions. As revealed above, ammonium phosphates were formed on the reactor wall when poisoning occurred under NH_3-SCR conditions, even though the phosphorus acid was injected directly into the heated reactor through a separate line. In order to facilitate a comparison of these different conditions, we examined the resulting P/Cu ratio and correlated that to the changes in the copper reduction property and the loss catalytic performances (i.e. deactivation). This will be thoroughly discussed in the following sections.

4.2. Influence of phosphorus on the copper reduction property

As disclosed by the H_2-TPR results, the peak reduction temperatures always shifted to higher temperatures on the samples from the inlets than those from the outlets. We speculate that such differences in the reduction temperatures among the samples from inlets and outlets mainly resulted from the axial distribution of P content. XPS results showed that copper metaphosphates were the main species after phosphorus poisoning (and subsequent pre-treatments and experiments). It has been reported that loading phosphorus on SiO_2-supported CuO leads to the reduction of copper shifts to a higher temperature [58,59]. In our previous work [41], where $(NH_4)_2HPO_4$ was used as a poison precursor for phosphorus poisoning of Cu-SSZ-13 powder catalysts, with 0.26 ~ 1.21 wt.% P, we found that a higher P loading on a sample led to a greater reduction of copper at higher temperatures (~490 °C) due to the formation of copper phosphates. Meanwhile, not all Cu ions could interact with the P species because phosphorus tended to form chain-like metaphosphate species inside the zeolite. In the present work, we have summarized the peak reduction temperatures from H_2-TPR profiles and their corresponding P/Cu ratios in the inlet and outlet parts of all phosphorus-poisoned samples, and the results are presented in Fig. 12. There is a clear correlation between peak reduction temperature and the P/Cu ratio. The peak reduction temperature of copper species shifted to a higher temperature by increasing the P/Cu ratio, but leveled at around 520 °C for high P loadings.

4.3. Correlation of P/Cu ratio to catalyst deactivation

4.3.1. NH_3 storage and NO storage

Our NH_3-TPD results showed an overall negative effect of

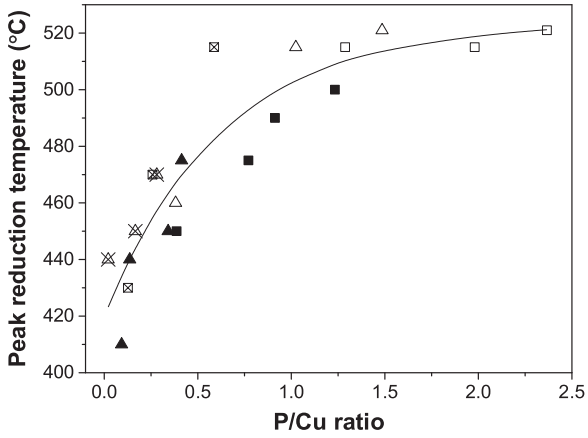

Fig. 12. Peak reduction temperature as a function of mean P/Cu ratio. The cubic and triangular symbols represent the samples from inlets and outlets, respectively. The solid, open, and open with × center symbols represent the samples poisoned under NH_3-free hydrothermal conditions at different poisoning temperatures, for different durations, and under NH_3-SCR operating conditions, respectively.

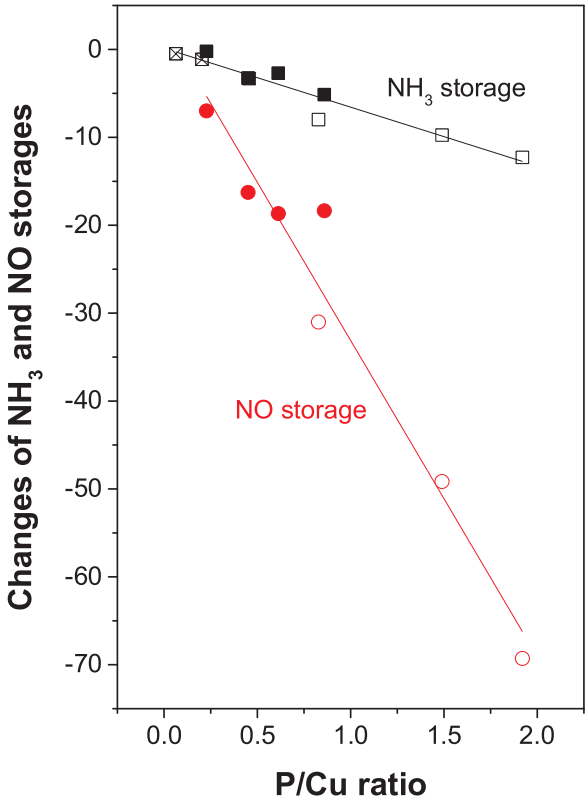

Fig. 13. Changes in total NH_3 storage (cubic) and NO storage (circle) as a function of mean P/Cu ratio. The solid, open, and open with × center symbols represent the samples poisoned under NH_3-free hydrothermal conditions at different poisoning temperatures, for different durations, and under NH_3-SCR operating conditions, respectively.

phosphorus on NH_3 storage, although only a minor effect under some conditions. The anchoring of P-species on either copper sites or a zeolite framework can occupy the acidic sites of NH_3 storage. In contrast, P-species also introduce new Brønsted acidic sites for storing NH_3 and, thereby, compensate the overall loss in NH_3 storage, especially for high-temperature stable, adsorbed species (S2). This hypothesis is strongly supported by the NH_3-TPD results in Section 3.1.2. The increase in NH_3 storage on S2 sites demonstrated that H_3PO_4-poisoning introduced new acidic sites onto the poisoned samples. A possible explanation for the enhanced high-temperature NH_3 storage ability, i.e., the new acidic sites, is that some of these anchoring P atoms might be associated with more acidic hydroxyl group in the form of P-OH, which will facilitate relatively strong coordination binding between NH_3 molecule and such acidic sites. This phenomenon was not observed in our previous work [39], where NH_3 storage on S1, S2, and S3 sites decreased when Cu-SSZ-13 catalysts were treated with $(NH_4)_2HPO_4$ with incipient wetness impregnation. This was probably because relatively low P loadings were used. Nevertheless, the overall NH_3 storage was reduced by the introduction of phosphorus. The trend displayed in Fig. 13 shows that the loss of total NH_3 storage was found to be linear as a function of the mean P/Cu ratio in the poisoned catalysts. This is in good agreement with our previous findings [39,41]. Moreover, the change in NO storage was also found to be linear as a function of the mean P/Cu ratio. It is noted that the impact of phosphorus on NO storage was significantly stronger than on NH_3 storage, indicating a larger contribution to catalyst deactivation during NH_3-SCR is the loss of NO storage.

4.3.2. NH_3 oxidation and NO oxidation

The correlations of P/Cu ratio to the deactivation of NH_3 and NO oxidation at 300 °C and 500 °C are shown in Fig. 14. The degree of deactivation caused by phosphorus poisoning on both NH_3 oxidation and NO oxidation increased with P/Cu ratio. The deactivation of both NH_3 and NO oxidation occurred rapidly with a P/Cu ratio up to 1.0 and, thereafter, leveled off. Interestingly, a similar relationship was found by correlating the P/Cu ratio with copper reduction temperature (Fig. 12), which strongly indicated that the deactivation of both NH_3 oxidation and NO oxidation was possibly due to the formation of copper phosphates. It has been reported in the literature that the Cu_xO_y species in the large cages in Cu-SSZ-13 are likely the active sites for NH_3 oxidation and NO oxidation [13,60]. We had demonstrated in our previous work [39,41], where Cu-SSZ-13 powder catalysts were impregnated with $(NH_4)_2HPO_4$ (yielded the P/Cu ratio 0.13 ~ 0.59), that phosphorus tends to react with copper sites and forms copper phosphates in the large cages, resulting in severe deactivation of both NH_3 oxidation and NO oxidation. Therefore, the rapid deactivation of NH_3 oxidation and NO oxidation depicted in Fig. 14 can be attributed to the strong interaction between phosphorus and copper sites in the large cages. When the P/Cu ratio is higher than 1.0, the blocking effect is built up by the continuing deposit of phosphorus in the pores and channels and, thus, hinders further increase in the interaction of phosphorus-copper.

4.3.3. Standard NH_3-SCR

Results of catalytic activity have shown that the impact of phosphorus is much more severe on NH_3 oxidation and NO oxidation reactions than on a standard NH_3-SCR reaction. The former reactions are typical side reactions that occur during the later reaction, especially at high reaction temperatures. Therefore, the influence of phosphorus on a standard NH_3-SCR reaction could be different. NH_3 oxidation and NO oxidation reactions are nearly inactive at the reaction temperature 200 °C. Therefore, a correlation of the P/Cu ratio with the deactivation at this reaction temperature is expected to reveal the real impact of phosphorus on the copper active sites for a standard NH_3-SCR reaction. As illustrated in Fig. 15 (lower panel), the deactivation of the NO_x reduction increased linearly with the P/Cu ratio at 200 °C. While at the reaction temperature of 250 °C (middle panel), the NO_x conversions were close to 100% on both fresh and Phosphorus-poisoned catalysts with a P/Cu ratio less than 1.0. Thus, these points cannot be used for studying the deactivation of NO_x reduction. Once the P/Cu ratio exceeds 1.0, the deactivation of NO_x reduction emerges, and the deactivation is linear with P/Cu ratio. It should be noted that the NH_3 and NO oxidation reactions at 250 °C were small, and the conversion of NH_3 or NO was less than 10% (see results in Section 3). The results demonstrate that the deactivation by phosphorus poisoning of a standard NH_3-SCR reaction linearly correlates with the total P content (or P/Cu ratio).

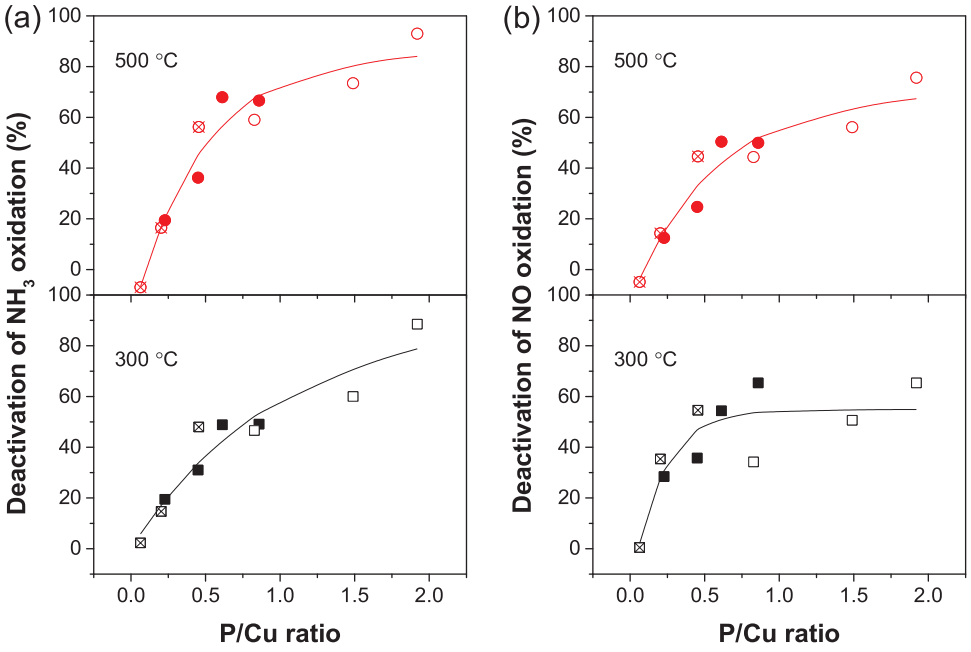

Fig. 14. Deactivation of NH_3 oxidation (a) and NO oxidation (b) as a function of mean P/Cu ratio at representative reaction temperatures: 300 °C and 500 °C. The solid, open, and open with × center symbols represent the samples poisoned under NH_3-free hydrothermal conditions at different poisoning temperatures, for different durations, and under NH_3-SCR operating conditions, respectively.

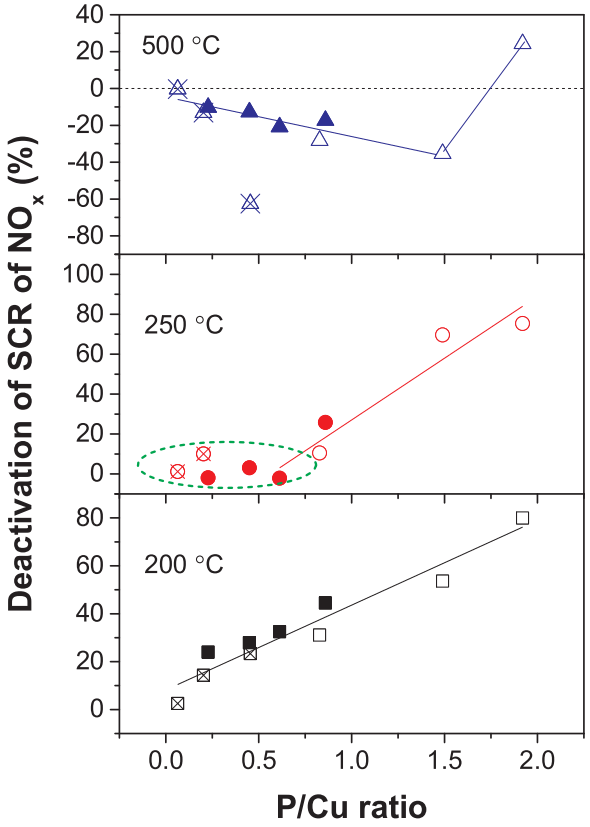

Fig. 15. of standard NH3-SCR of NOx as a function of mean P/Cu ratio at representative reaction temperatures: 200 °C, 250 °C, and 500 °C. The solid, open, and open with × center symbols represent the samples poisoned under NH3-free hydrothermal conditions at different poisoning temperatures, for different durations, and under NH3-SCR operating conditions, respectively.Deactivation Fig. 15gr15of standard NH_3-SCR of NO_x as a function of mean P/Cu ratio at representative reaction temperatures: 200 °C, 250 °C, and 500 °C. The solid, open, and open with × center symbols represent the samples poisoned under NH_3-free hydrothermal conditions at different poisoning temperatures, for different durations, and under NH_3-SCR operating conditions, respectively.

There are quite a few studies in the literature reported the relationship of P loading with activity loss on poisoned catalysts. Silver, et al. [61] have found that the decrease in SCR performance over Fe/zeolites is proportional to the P loading on the poisoned catalysts. In addition to phosphorus poisoning, Janssens and coworkers have recently found that sulfur poisoning causes irreversible and reversible deactivation on Cu-CHA SCR catalysts and the irreversible deactivation is proportional to the sulfur content that remains after regeneration at 550 °C [36].

At 500 °C, the NH_3 oxidation becomes very active and decreases the supply of NH_3 for NO_x reduction. As shown in the results of NH_3-SCR in Section 3, a low P content (i.e. low P/Cu ratio) on poisoned catalysts could suppress NH_3 oxidation and improve the efficiency for NO_x reduction. It was found that the enhancement of NO_x reduction at 500 °C can be maintained at a P/Cu ratio as high as 1.5. When the P/Cu ratio exceeds 1.5, the active sites for NO_x reduction are blocked by a massive deposit of phosphorus, leading to a deactivation of SCR performance at high temperatures (e.g. 500 °C).

4.4. Phosphorus inhibition of N_2O emission

N_2O, which is a greenhouse gas, is one of the side-products during the NH_3-SCR over Cu-zeolites. Despite that Cu-SSZ-13 catalysts have lower N_2O selectivity than Cu/BEA catalysts [62,63], N_2O formation has attracted increasing attention due to concerns about this substance. Our observations (Figs. S5, S7, S11, S13, Fig. S16 and S18) show that N_2O is produced during the ammonia oxidation that follows the reaction described in Eq. 5, and it is also produced during the NH_3-SCR that follows the reaction described in Eq. 6 [64].

$$2NH_3 + 2O_2 \rightarrow N_2O + 3H_2O \quad (5)$$

$$2NO + 2NH_3 + O_2 \rightarrow N_2 + N_2O + 3H_2O \quad (6)$$

The concentrations of N_2O during NH_3 oxidation are barely over 3 ppm, which is much lower than those produced during NH_3-SCR (maximum near 8 ppm). On the other hand, the N_2O during NH_3 oxidation is produced mainly at the reaction temperature of 300 °C, while it is mainly produced at 200 °C during standard NH_3-SCR operating conditions. This indicates that the formation of N_2O during standard NH_3-SCR operating conditions is highly relevant for the decomposition of NH_4NO_3 precursor species, which possibly involves NO oxidation to NO_2 [65]. Our findings show that phosphorus strongly inhibits the

formation of N_2O during standard NH_3-SCR operating conditions, indicating that phosphorus possibly suppresses the formation or decomposition of the NH_4NO_3 intermediate.

5. Conclusions

To elucidate the deactivation of Cu-SSZ-13 NH_3-SCR catalysts with phosphorus, catalysts were exposed to H_3PO_4 vapor-containing flows under NH_3-free lean hydrothermal conditions (100 ppm H_3PO_4, 5 vol.% H_2O, 8 vol.% O_2, and Ar) and NH_3-SCR operating conditions (100 ppm H_3PO_4, 400 ppm NH_3, 400 ppm NO, 5 vol.% H_2O, 8 vol.% O_2, and Ar), respectively. Three types of phosphorus species on the spent poisoned catalysts were determined with XPS analysis: phosphorus oxide (P_2O_5), metaphosphate (PO_3^-), and phosphate (PO_4^{3-}). Metaphosphate was identified as the dominant compound. The axial distribution analysis with both XPS and ICP-SFMS revealed that phosphorus was mainly captured at the inlets. The radial distribution analysis under SEM observation showed a larger phosphorus gradient from the washcoat surface to the bulk with a shorter duration of poisoning and a smaller gradient with a longer duration of poisoning. The H_2-TPR study demonstrated that phosphorus induces shifts in the peak copper reduction to a higher temperature and the temperature shift was strongly correlated with the P/Cu ratio.

The catalytic activities (including NH_3 and NO storages, NH_3 oxidation, NO oxidation, and standard NH_3-SCR) before and after phosphorus poisoning under different poisoning conditions were compared to evaluate the influence of phosphorus on Cu-SZZ-13 as an NH_3-SCR catalyst. The deactivation of NH_3 oxidation and NO oxidation strongly increased with the P/Cu ratio and levels of at high P/Cu ratios, with a trend similar to the temperature for copper reduction. However, the deactivations in NH_3 and NO storage and standard NH_3-SCR were proportional to the P/Cu ratio. The phosphorus inhibition of NO storage was significantly stronger than that for NH_3 storage, indicating that the deactivation of NH_3-SCR performance partially attributed to the decreased capacity of chemisorbed NO. The H_3PO_4 poisoning experiments implemented under NH_3-free lean hydrothermal conditions yielded relatively high P captured on the monolith catalysts, and the poisoned catalysts showed remarkable loss in oxidation reactions. The deactivation of the standard SCR reaction was smaller after poisoning, but for long durations (e.g. 34 h) significant deactivation of the ammonia SCR functions was also found.

Acknowledgements

This study was performed at the Division of Chemical Engineering and the Competence Centre for Catalysis, Chalmers University of Technology, in collaboration with Cummins Inc. The financial support from Cummins Inc. and the Swedish Research Council (642-2014-5733) are gratefully acknowledged.

Appendix A. Supplementary data

Supplementary material related to this article can be found, in the online version, at doi:https://doi.org/10.1016/j.apcatb.2019.117815.

References

[1] W. Held, A. König, T. Richter, L. Puppe, Catalytic NO_x reduction in net oxidizing exhaust gas, SAE Int. J. Fuels Lubr. 99 (1990) 209–216.
[2] P.L.T. Gabrielsson, Urea-SCR in automotive applications, Top. Catal. 28 (2004) 177–184.
[3] I. Nova, E. Tronconi, Urea-SCR Technology for deNO_x After Treatment of Diesel Exhausts, Springer, New York, 2014.
[4] A.K. Ingole, D. Dixit, S.V. Dingare, A review on Selective Catalytic Reduction technique for diesel engine exhaust after treatment, Int. J. Curr. Eng. Tech. (2017) 206–210.
[5] T. Johnson, A. Joshi, Review of Vehicle Engine Efficiency and Emissions, SAE Tech. Pap. 2018-2001-0329 (2018) https://doi.org/10.1016/2010.4271/2018-2001-0329.
[6] T. Maunula, T. Kinnunen, M. Iivonen, Design and Durability of Vanadium-SCR Catalyst Systems in Mobile Off-Road Applications, SAE Tech. Pap. 2011-2001-1316 (2011) https://doi.org/10.1016/2010.4271/2011-2001-1316.
[7] S. Brandenberger, O. Krocher, A. Tissler, R. Althoff, The state of the art in selective catalytic reduction of NOx by ammonia using metal-exchanged zeolite catalysts, Catal. Rev.-Sci. Eng. 50 (2008) 492–531.
[8] Y. Xin, Q. Li, Z.L. Zhang, Zeolitic materials for deNO_x selective catalytic reduction, ChemCatChem 10 (2018) 29–41.
[9] A.M. Beale, F. Gao, I. Lezcano-Gonzalez, C.H.F. Peden, J. Szanyi, Recent advances in automotive catalysis for NO_x emission control by small-pore microporous materials, Chem. Soc. Rev. 44 (2015) 7371–7405.
[10] F. Gao, J.H. Kwak, J. Szanyi, C.H.F. Peden, Current understanding of Cu-Exchanged chabazite molecular sieves for use as commercial diesel engine deNO_x catalysts, Top. Catal. 56 (2013) 1441–1459.
[11] J.H. Wang, H.W. Zhao, G. Haller, Y.D. Li, Recent advances in the selective catalytic reduction of NOx with NH_3 on Cu-Chabazite catalysts, Appl. Catal. B 202 (2017) 346–354.
[12] K. Leistner, A. Kumar, K. Kamasamudram, L. Olsson, Mechanistic study of hydrothermally aged Cu/SSZ-13 catalysts for ammonia-SCR, Catal. Today 307 (2018) 55–64.
[13] L. Olsson, K. Wijayanti, K. Leistner, A. Kumar, S.Y. Joshi, K. Kamasamudram, N.W. Currier, A. Yezerets, A multi-site kinetic model for NH_3-SCR over Cu/SSZ-13, Appl. Catal. B 174 (2015) 212–224.
[14] K. Leistner, C. Gonzalez Braga, A. Kumar, K. Kamasamudram, L. Olsson, Volatilisation and subsequent deposition of platinum oxides from diesel oxidation catalysts, Appl. Catal. B 241 (2019) 338–350.
[15] J. Granestrand, S. Dahlin, O. Immele, L. Schmalhorst, C. Lantto, M. Nilsson, R.S. París, F. Regali, L.J. Pettersson, Catalytic aftertreatment systems for trucks fueled by biofuels - aspects on the impact of fuel quality on catalyst deactivation, Catalysis 30 (2018) 64–145. The Royal Society of Chemistry.
[16] M.J. Rokosz, A.E. Chen, C.K. Lowe-Ma, A.V. Kucherov, D. Benson, M.C.P. Peck, R.W. McCabe, Characterization of phosphorus-poisoned automotive exhaust catalysts, Appl. Catal. B-Environ. 33 (2001) 205–215.
[17] B.G. Bunting, K. More, S. Lewis, T. Toops, Phosphorous Poisoning and Phosphorous Exhaust Chemistry with Diesel Oxidation Catalysts, SAE Tech. Pap. 2005-2001-1758 (2005) https://doi.org/10.1016/2010.4271/2005-2001-1758.
[18] S.A. Culley, T.F. McDonnell, The Impact of Passenger Car Motor Oil Phosphorus Levels on Engine Durability, Oil Degradation, and Exhaust Emissions in a Field Trial, SAE Tech. Pap. 952344 (1995) https://doi.org/10.1016/952310.954271/952344.
[19] S.A. Culley, T.F. McDonnell, D.J. Ball, C.W. Kirby, S.W. Hawes, The impact of passenger car motor oil phosphorus levels on automotive emissions control systems, SAE Int. J. Fuels Lubr. 105 (1996) 1216–1225.
[20] D.D. Beck, J.W. Sommers, C.L. DiMaggio, D.R. Monroe, D.A. Frank, Impact of oil-derived catalyst poisons on FTP performance of LEV catalyst systems, SAE Int. J. Fuels Lubr. 106 (1997) 916–925.
[21] S. Dahlin, M. Nilsson, D. Backstrom, S.L. Bergman, E. Bengtsson, S.L. Bernasek, L.J. Pettersson, Multivariate analysis of the effect of biodiesel-derived contaminants on V_2O_5-WO_3/TiO_2 SCR catalysts, Appl. Catal. B 183 (2016) 377–385.
[22] H.N. Masahito Shibata, Shigeki Takeshima, Koji Hoshino, A study of engine oil composition effects on zeolite-type SCR catalyst durability, SAE J. (2007) 2042–2051 2007-01-1924.
[23] S.J. Eaton, B.G. Bunting, T.J. Toops, K. Nguyen, The Roles of Phosphorus and Soot on the Deactivation of Diesel Oxidation Catalysts, SAE International, 2009.
[24] T.L.a.H.S.H, Youngjin Cho, Jae Au Ha, Deactivation of urea SCR catalyst for heavy duty diesel engine, SAE Int. (2012) 2012-01-1956.
[25] G.C. Bond, S.F. Tahir, Influence of phosphorus and potassium additives on the properties of vanadia/titania catalysts, Catal. Today 10 (1991) 393–395.
[26] N.Z. Yang, R.T. Guo, Q.S. Wang, W.G. Pan, Q.L. Chen, C.Z. Lu, S.X. Wang, Deactivation of Mn/TiO_2 catalyst for NH_3-SCR reaction: effect of phosphorous, RSC Adv. 6 (2016) 11226–11232.
[27] V. Kröger, M. Hietikko, U. Lassi, J. Ahola, K. Kallinen, R. Laitinen, R.L. Keiski, Characterization of the effects of phosphorus and calcium on the activity of Rh-containing catalyst powders, Top. Catal. 30–31 (2004) 469–473.
[28] V. Kröger, T. Kanerva, U. Lassi, K. Rahkamaa-Tolonen, M. Vippola, R.L. Keiski, Characterization of phosphorus poisoning on diesel exhaust gas catalyst components containing oxide and Pt, Top. Catal. 45 (2007) 153–157.
[29] S. Andonova, E. Vovk, J. Sjöblom, E. Ozensoy, L. Olsson, Chemical deactivation by phosphorous under lean hydrothermal conditions over Cu/BEA NH_3-SCR catalysts, Appl. Catal. B 147 (2014) 251–263.
[30] S. Shwan, J. Jansson, L. Olsson, M. Skoglundh, Deactivation mechanisms of iron-exchanged zeolites for NH_3-SCR applications, Catal. Today 258 (2015) 432–440.
[31] V. Kröger, M. Hietikko, D. Angove, D. French, U. Lassi, A. Suopanki, R. Laitinen, R.L. Keiski, Effect of phosphorus poisoning on catalytic activity of diesel exhaust gas catalyst components containing oxide and Pt, Top. Catal. 42–43 (2007) 409–413.
[32] V. Kröger, T. Kanerva, U. Lassi, K. Rahkamaa-Tolonen, T. Lepisto, R.L. Keiski, Phosphorus poisoning of ZSM-5 and Pt/ZSM-5 zeolite catalysts in diesel exhaust gas conditions, Top. Catal. 42–43 (2007) 433–436.
[33] A. Kumar, M.A. Smith, K. Kamasamudram, N.W. Currier, H. An, A. Yezerets, Impact of different forms of feed sulfur on small-pore Cu-zeolite SCR catalyst, Catal. Today 231 (2014) 75–82.
[34] L. Olsson, K. Wijayanti, K. Leistner, A. Kumar, S.Y. Joshi, K. Kamasamudram, N.W. Currier, A. Yezerets, A kinetic model for sulfur poisoning and regeneration of Cu/SSZ-13 used for NH_3-SCR, Appl. Catal. B 183 (2016) 394–406.
[35] K. Wijayanti, K.P. Xie, A. Kumar, K. Kamasamudram, L. Olsson, Effect of gas

compositions on SO_2 poisoning over Cu/SSZ-13 used for NH3-SCR, Appl. Catal. B-Environ. 219 (2017) 142–154.
[36] P.S. Hammershøi, Y. Jangjou, W.S. Epling, A.D. Jensen, T.V.W. Janssens, Reversible and irreversible deactivation of Cu-CHA NH_3-SCR catalysts by SO_2 and SO_3, Appl. Catal. B 226 (2018) 38–45.
[37] Y. Jangjou, Q. Do, Y.T. Gu, L.G. Lim, H. Sun, D. Wang, A. Kumar, J.H. Li, L.C. Grabow, W.S. Epling, Nature of Cu active centers in Cu-SSZ-13 and their responses to SO_2 exposure, ACS Catal. 8 (2018) 1325–1337.
[38] I. Lezcano-Gonzalez, U. Deka, H.E. van der Bij, P. Paalanen, B. Arstad, B.M. Weckhuysen, A.M. Beale, Chemical deactivation of Cu-SSZ-13 ammonia selective catalytic reduction (NH_3-SCR) systems, Appl. Catal. B 154 (2014) 339–349.
[39] K.P. Xie, K. Leistner, K. Wijayanti, A. Kumar, K. Kamasamudram, L. Olsson, Influence of phosphorus on Cu-SSZ-13 for selective catalytic reduction of NO_x by ammonia, Catal. Today 297 (2017) 46–52.
[40] Z. Chen, C. Fan, L. Pang, S. Ming, P. Liu, T. Li, The influence of phosphorus on the catalytic properties, durability, sulfur resistance and kinetics of Cu-SSZ-13 for NO_x reduction by NH_3-SCR, Appl. Catal. B 237 (2018) 116–127.
[41] K. Xie, J. Woo, D. Bernin, A. Kumar, K. Kamasamudram, L. Olsson, Insights into hydrothermal aging of phosphorus-poisoned Cu-SSZ-13 for NH_3-SCR, Appl. Catal. B (2018), https://doi.org/10.1016/j.apcatb.2018.1008.1082.
[42] S. Shwan, J. Jansson, L. Olsson, M. Skoglundh, Chemical deactivation of Fe-BEA as NH_3-SCR catalyst-Effect of phosphorous, Appl. Catal. B-Environ. 147 (2014) 111–123.
[43] J.F. Moulder, W.F. Stickle, P.E. Sobol, K.D. Bomben, Handbook of X-Ray Photoelectron Spectroscopy, Perkin-Elmer Corp., Eden Prairie, Minnesota, 1992.
[44] J.M. Guevremont, G. Guinther, T.-C. Jao, T. Herlihy, R. White, J. Howe, Total Phosphorus Detection and Mapping in Catalytic Converters, SAE Tech. Pap. 2007-2001-4078 (2007) https://doi.org/10.1016/2010.4271/2007-2001-4078.
[45] M. Nagata, Y. Tanaka, Modeling of Phosphorus Poisoning Phenomena over Diesel Oxidation Catalysts, SAE Tech. Pap. 2010-2001-0884 (2010) https://doi.org/10.1016/2010.4271/2010-2001-0884.
[46] S. Malmberg, M. Votsmeier, J. Gieshoff, N. Söger, L. Mußmann, A. Schuler, A. Drochner, Dynamic phenomena of SCR-catalysts containing Fe-exchanged zeolites – experiments and computer simulations, Top. Catal. 42 (2007) 33–36.
[47] L. Olsson, H. Sjövall, R.J. Blint, A kinetic model for ammonia selective catalytic reduction over Cu-ZSM-5, Appl. Catal. B 81 (2008) 203–217.
[48] S. Shwan, J. Jansson, J. Korsgren, L. Olsson, M. Skoglundh, Kinetic modeling of H-BEA and Fe-BEA as NH3-SCR catalysts-Effect of hydrothermal treatment, Catal. Today 197 (2012) 24–37.
[49] K. Leistner, K.P. Xie, A. Kumar, K. Kamasamudram, L. Olsson, Ammonia desorption peaks can Be assigned to different copper sites in Cu/SSZ-13, Catal. Lett. 147 (2017) 1882–1890.
[50] J. Szanyi, J.H. Kwak, H.Y. Zhu, C.H.F. Peden, Characterization of Cu-SSZ-13 NH_3 SCR catalysts: an *in situ* FTIR study, Phys. Chem. Chem. Phys. 15 (2013) 2368–2380.
[51] R.Q. Zhang, J.S. McEwen, M. Kollár, F. Gao, Y.L. Wang, J. Szanyi, C.H.F. Peden, NO chemisorption on Cu/SSZ-13: a comparative study from infrared spectroscopy and DFT calculations, ACS Catal. 4 (2014) 4093–4105.
[52] R. Jonsson, O. Mihai, J. Woo, M. Skoglundh, E. Olsson, M. Berggrund, L. Olsson, Gas-phase phosphorous poisoning of a $Pt/Ba/Al_2O_3$ NO_x storage catalyst, Catalysts 8 (2018), https://doi.org/10.3390/catal8040155.
[53] F. Castellino, S.B. Rasmussen, A.D. Jensen, J.E. Johnsson, R. Fehrmann, Deactivation of vanadia-based commercial SCR catalysts by polyphosphoric acids, Appl. Catal. B 83 (2008) 110–122.
[54] P.W. Atkins, T.L. Overton, J.P. Rourke, M.T. Weller, F.A. Armstrong, Shriver and Atkins' Inorganic Chemistry, fifth edition, Oxford University Press, New York, 2010.
[55] W.B. Williamson, J. Perry, H.S. Gandhi, J.L. Bomback, Effects of oil phosphorus on deactivation of monolithic three-way catalysts, Appl. Catal. 15 (1985) 277–292.
[56] L.L. Hegedus, K. Baron, Phosphorus accumulation in automotive catalysts, J. Catal. 54 (1978) 115–119.
[57] H. Sumida, Y. Koda, A. Sadai, S. Ichikawa, M. Kyogoku, M. Takato, Y. Miwa, R.W. McCabe, Analysis of Phosphorus Poisoning on Exhaust Catalysts from Compact-Class Vehicle, SAE Tech. Pap. 2004-2001-0147 (2004) https://doi.org/10.1016/2010.4271/2004-2001-0147.
[58] G.V. Mamontov, O.V. Magaev, A.S. Knyazev, O.V. Vodyankina, Influence of phosphate addition on activity of Ag and Cu catalysts for partial oxidation of alcohols, Catal. Today 203 (2013) 122–126.
[59] C. Sepúlveda, L. Delgado, R. García, M. Melendrez, J.L.G. Fierro, I.T. Ghampson, N. Escalona, Effect of phosphorus on the activity of Cu/SiO_2 catalysts in the hydrogenolysis of glycerol, Catal. Today 279 (2017) 217–223.
[60] A.A. Verma, S.A. Bates, T. Anggara, C. Paolucci, A.A. Parekh, K. Kamasamudram, A. Yezerets, J.T. Miller, W.N. Delgass, W.F. Schneider, F.H. Ribeiro, NO oxidation: a probe reaction on Cu-SSZ-13, J. Catal. 312 (2014) 179–190.
[61] R.G. Silver, M.O. Stefanick, B.I. Todd, A study of chemical aging effects on HDD Fe-zeolite SCR catalyst, Catal. Today 136 (2008) 28–33.
[62] H.Y. Chen, Z.H. Wei, M. Kollar, F. Gao, Y.L. Wang, J. Szanyi, C.H.F. Peden, A comparative study of N_2O formation during the selective catalytic reduction of NOx with NH3 on zeolite supported Cu catalysts, J. Catal. 329 (2015) 490–498.
[63] K. Leistner, O. Mihai, K. Wijayanti, A. Kumar, K. Kamasamudram, N.W. Currier, A. Yezerets, L. Olsson, Comparison of Cu/BEA, Cu/SSZ-13 and Cu/SAPO-34 for ammonia-SCR reactions, Catal. Today 258 (2015) 49–55.
[64] G. Madia, M. Koebel, M. Elsener, A. Wokaun, Side reactions in the selective catalytic reduction of NO_x with various NO_2 fractions, Ind. Eng. Chem. Res. 41 (2002) 4008–4015.
[65] T.V.W. Janssens, H. Falsig, L.F. Lundegaard, P.N.R. Vennestrøm, S.B. Rasmussen, P.G. Moses, F. Giordanino, E. Borfecchia, K.A. Lomachenko, C. Lamberti, S. Bordiga, A. Godiksen, S. Mossin, P. Beato, A consistent reaction scheme for the selective catalytic reduction of nitrogen oxides with ammonia, ACS Catal. 5 (2015) 2832–2845.